RICE UNIVERSITY

Modeling Curved Movement

By

Melissa Ann Gallagher

A THESIS SUBMITTED
IN PARTIAL FULFILLMENT OF THE
REQUIREMENT FOR THE DEGREE

Master of Arts

Approved, Thesis Committee:

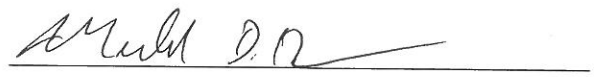

Michael D. Byrne, Professor,
Psychology

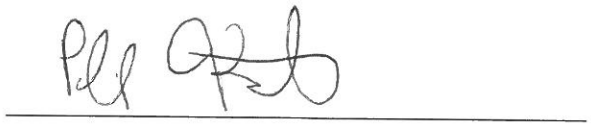

Philip T. Kortum, Assistant Professor,
Psychology

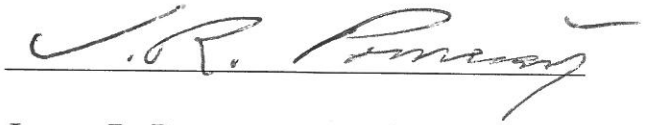

James R. Pomerantz, Professor,
Psychology

Houston, Texas
January 2013

ABSTRACT

Modeling Curved Movement

by

Melissa A. Gallagher

This work aims to further the understanding of the trajectory and velocity profile of curved motion. Two competing theories, the two-thirds power law and the minimum jerk velocity profile, were tested. Two experiments were run that had the subjects generate curved motion. The first experiment had subjects move along a bounded ellipse and the second experiment had subjects move in a less constrained manner inducing a curved path. The study shows evidence for the expected effects of distance traveled and allowable room for error. There is little evidence for the two movement profiles explaining the data.

ACKNOWLEDGEMENTS

This work would not have been possible without the guidance and mentorship of my advisor, Dr. Michael D. Byrne. I would like to thank my committee members, Dr. Philip T. Kortum and Dr. James R. Pomerantz, for their support and feedback; our collaborators in the MAHI lab, specifically Dr. Marcia O'Malley and Sagar Neel Purkayastha for their aid in the initial work on the spring-target task. Finally I would like to thank my friends, family, and lab mates for their support and encouragement.

TABLE OF CONTENTS

LIST OF TABLES

LIST OF FIGURES

Modeling Curved Movement

Much of the motor movement research in human-computer interaction has focused on Fitts's law and extensions to it. A richer understanding of human motor movement is needed as interfaces extend beyond the point-and-click paradigm. As drawing, writing, and interfacing with a three-dimensional space become more common, ways to model these types of movement become necessary. The goal of this research is to evaluate models of curved movement in a two-dimensional space. In order to achieve this goal, a specific motor movement task will be discussed. The task has reflected on shortcomings in the ability to model certain types of human motor movement. The initial work that was done to expand the model of aimed movement will be explained. Finally, the current models of curved movement in a two dimensional space will be discussed. Past work using these models informed the design of two experiments. The data from the experiments were evaluated against the models to see if either model could expand the ability to create a cognitive model of curved movement on the experimental tasks, as well as the original task.

The particular human motor movement task, the spring-target task, has been studied extensively by O'Malley and colleagues. (O'Malley, et al., 2006; Li, Patoglu, & O'Malley, 2009; Huegel, et al., 2009, Powell, 2010) The spring-target task was an ideal task to model with Fitts's Law because a specific group of participants completed the task by making aimed movements. This motor control task is based on a spring-target system (Figure 1). There are two stationary targets on the screen. One is positioned in the lower left corner; the other is positioned in the upper right corner. The goal is to hit the targets in an alternating pattern with a disc. The disc is connected to a tool by a damped spring. The tool is visually represented as a circle of a different color than the disc, which the operator controls. This task is not a tracking task because the

targets are stationary. The task is scored on how many hits the subject can get in a 20 second interval.

The work done by O'Malley et. al. initially focused on different training methods to improve the subjects' performance. Some of the methods that were employed were haptic feedback and visual cues. The results of the training studies did not support any one particular training method as beneficial compared to the others. However, the studies produced an interesting pattern of subjects' strategy learning over the sessions.

When the data of the subjects' hit performance was analyzed, three distinct groups appeared (Figure 2). The first group of subjects was the high performers. High performers are classified as such if their initial performance was one standard deviation above the mean. The subjects in this group started out with good performance on the task and their performance also showed a pattern of linear improvement over sessions. The movement profile for the high performers suggested that they moved along the target axis with minimal off-axis motion, exploiting the physics of the system to improve their performance. Fitts's Law is a model for this type of straight-line aimed movement. The second group was the low performers. Low performers were classified as such if their final score fell below one standard deviation from the mean. The subjects in this group started out with poor performance on the task and their performance improved linearly over the sessions, but they were never able to perform as well as the subjects in the other two groups. The movement profile for the low performers suggested that they tended to make circular movements around the field, effectively swinging the coupled mass around to hit the targets. The third group of subjects was classified as the transitional performers. This group started out with performance comparable to the low performers but ended up with performance comparable to the high performers. The learning curve that the transitional

performers exhibited was better fit by a logarithmic function than a linear one. The movement profiles for the transitional performers started similarly to the low performers and end up similarly to the high performers. What information the transitional subjects learned to change their performance from a low performance to high performance is currently an open question. The three performance groups naturally formed in spite of the fact that all subjects were given the same instructions for optimal performance on the task.

To model this task the modeling language ACT-R was used. ACT-R (Anderson, 2007) is a multi-domain cognitive architecture for simulating and understanding human cognition. The learning procedure for ACT-R was well suited to this task while the ability to model continuous motor movement was not. ACT-R was not designed for and has not been applied to many continuous motor tasks, so modifications were made so that ACT-R could perform this task. To model the low performers more extensions to ACT-R will be necessary due to the different nature of their movement, specifically that it is curved, unlike the high performers whose movement is linear. Fitts's law and the minimum jerk velocity profile were the two theories that informed how the high performer's movements were modeled. These theories and the modifications to ACT-R are discussed in detail.

Fitts (1954) first applied information theory to the human motor system with his research into pointing tasks. Three experimental tasks were used to quantify this relationship. Three distinct tasks; bar strip tapping, disk transfer, and nail insertion, were all part of an overarching goal of hitting a target at a specified distance. From these tasks Fitts formalized the relationship of the speed/accuracy trade off in the aimed movement.

$$T = a + b\ log_2\left(\frac{2A}{W}\right) \qquad (1)$$

The model predicts that the time needed to point to a target of width *W* at a distance of *A* is logarithmically related to the inverse of the relationship between the two. The values *a* and *b* are empirically derived constants. The *log* portion of Fitts's law quantifies the index of difficulty for a task. The larger the value the harder it is for a subject to perform the task. The index of difficulty is a main advantage of Fitts's law as it allows specific movements to be translated to a performance index, which can be used to compare device performance across tasks. The original formulation, Equation 1, has been modified so that the log portion is $A/W + c$, where *c* is usually 1 (MacKenzie 1992). While Fitts's law quantifies the speed-accuracy trade off in movement it gives no information regarding the velocity and trajectory of the movement. Fitts's law is also limited in its ability to evaluate devices in tasks that are not pointing tasks.

Flash and Hogan (1985) studied the velocity profile of voluntary human arm movements and quantified it with the minimum jerk movement profile. The task paradigms examined free movement of the hand toward a goal in the horizontal plane, which is similar to the paradigm that Fitts used. "Studies showed that when moving the hand between pairs of targets; subjects tended to generate roughly straight hand trajectories with single-peaked, bell-shaped speed profiles independent of the workspace in which the movement was formed."(Flash and Hogan, 1984 pg 1688). The minimum jerk movement profile hypothesizes that the most effective way to move smoothly from one point to another is to minimize the sum of the squared jerk along the trajectory. The jerk is defined as the third derivative of position. Hogan proposed that a function that connects two points in a certain amount of time would be quantified with the minimum jerk cost. Using optimization theory all trajectories that would connect these two points within the time constraint are examined and the one with the minimum jerk cost is used. The general form of the velocity of movement under this theory is bell shaped with a single maximum of velocity.

An example movement and the velocity of the movement are shown in Figure 3. The general equation (2) predicts minimum jerk movement where *T* is the duration of movement.

$$C_3 = \int_0^T dt \left(\left(\frac{d^3x}{dt^3} \right)^2 + \left(\frac{d^3y}{dt^3} \right)^2 \right) \quad (2)$$

Combining Fitts's law and the minimum jerk movement profile predicts a movement trajectory in a pointing task. Fitts's law calculates the time to move to a target a specified distance away. The minimum jerk movement profile then takes this time and the distance and computes the velocity profile. This is useful in implementing a model of continuous movement along a path. These modifications were made to ACT-R to change the way that it moved the mouse and the output of the aimed movement (Byrne et. al. 2010). ACT-R's original system for movement calculated the movement time based on Fitts's law and then, when the movement time had elapsed, instantaneously moved the mouse to the new location. With a physics-based system, like the spring-target task, this type of movement produces infinite acceleration that over-excites the system. ACT-R's motor module was modified to output positional data in 3 ms intervals so the physics of the system would react to the models movements similarly to the subjects' movements. The next modification that was made to ACT-R was to the velocity profile of the movement. ACT-R was originally programed to move at a constant velocity for the duration of the movement and when the movement ended return the velocity to zero. This is not a realistic representation for the task because the acceleration would jump from zero to a constant at the beginning of the movement and then back from a constant to zero at the end. The linear function for velocity was replaced by the "minimum jerk" movement profile (Hogan, 1984). The minimum jerk profile is smoother than human performance (cf. Jagacinski & Flach, 2003), which tends to involve small velocity corrections over the course of movement, but the approximation is close enough, and also fast and easy to compute. With these modifications to

ACT-R in place, a model of the high performers in the spring-target task was constructed. The model does not encompass all elements of the task but generates a hit count similar to the subjects.

Continuing in this line of research, the extension of information theory and the speed accuracy trade off has advanced beyond simply pointing tasks. Based on the Fitts's law, Accot and Zhai (1997) quantified movement time through bounded trajectories of any shape in what has become known as the steering law. The generic expression of the index of difficulty becomes Equation (3) so the time predictions are modeled by equation (4). Equation (3) is analogous to the log portion of Equation (1) and is comparable across tasks with out being restricted to linear movement. Equation (4) is the full form of Fitts's law with the new index of difficulty added in.

$$ID_C = \int_C \frac{ds}{W(s)} \tag{3}$$

$$T_C = a + b \int_C \frac{ds}{W(s)} \tag{4}$$

These equations were mathematically derived and then empirically tested on tasks of increasing complexity. The first task used was a goal-passing task, where subjects only had to pass through goals of a fixed width at the beginning and end of the task (Figure 4). The constraints were then increased so that subjects had to move along a straight tunnel (Figure 5). The two most difficult tasks were a narrowing tunnel task (Figure 6) and a spiral tunnel task (Figure 7). The steering law had high predictive value for completion time in all the tasks studied, with all correlations greater than .96. This work has been applied to navigating hierarchical menus in a graphic user interface and can be used to compare devices on more than just pointing tasks. Having an extension to Fitts's law that models curved movement will also be helpful in modeling the low performers on the spring-target task.

While the steering law has the ability to predict movement time for a curved path, there are competing theories as to the best way to model the velocity. Both the minimum jerk movement profile and the two-thirds power law have been used to describe different classes of curved movement. The minimum jerk movement profile has found success in single curved movements as well as curved movements through specified points. The two-thirds power law has had move success in tracing tasks.

In Flash and Hogan's (1985) study curved movement was also examined. While curved movement did not generate a velocity profile with a bell shaped curve with a single maximum (Figure 3), the hand paths were still smooth (Figure 8). There was a relationship between the location of the minima in the velocity profile and the peaks in the curvature of the path. The assumption became that the hand had to travel through a specified intermediate point, which caused the minima in the profile. This point is not specified a priori but is determined during the optimization procedure. The theory behind this is similar to the theory behind the steering law. The steering law is broken up subcomponents of Fitts's law and integrated across the entire path. The extension to the minimum jerk profile to account for curved movement breaks the movement up into sub movements based on the curves in the path and sums them together. This extension to the minimum jerk profile with an unspecified waypoint point had both good quantitative and qualitative fit. Todorov and Jordan (1998) extended the work on the minimum jerk profile for curved movement. They wrote an algorithm that generates an optimized velocity profile of curved movement through any set of points given the completion time and a set of waypoints. The algorithm explained up to 95% of the variance of the velocity profile of the subjects in their experiments.

A second theory of curved movement accounts for the relationship between the geometrical and kinematic properties of movement trajectories. This theory is called the two-thirds power law. This law states that the angular velocity of the hand is proportional to the two-thirds root of its curvature (Viviani and Terzuolo, 1982; Lacquaniti et al., 1983). Equivalently the instantaneous tangential velocity is proportional to the third root of the radius of curvature. The general form equation is equation (5) where *v* is tangential velocity, *k* is curvature as calculated by equation (6), *g* is the experimentally derived gain factor that describes the tempo of movement, and *–b* is approximately 0.33.

$$v = g\, k^{-b} \tag{5}$$

$$k = \frac{|v_x a_y - v_y a_x|}{(V_x^2 + V_y^2)^{3/2}} \tag{6}$$

This formulation has been used extensively in tracing tasks. Primarily the tracing of ellipses has been the paradigm but to a lesser extent tracing complex shapes. A constant gain factor has not always been able to account for the variation of velocity across movement and a piecewise gain factor has been used to explain the segmentation of movement.

To continue expanding ACT-R's motor module a better understanding of curved motor movement is needed. To compare the two-thirds power law with the minimum jerk movement profile, two new tasks were devised to collect trajectory and time data. The first task tested movement along a bounded elliptical path. The second task does not contain a bounded path but still constrains subjects to make similar movements to the first experiment hoping to elicit curved movements.

EXPERIMENT ONE

The first experiment was designed to test the subject's movement through a bounded path. There are different levels and manipulation of the independent variables to create different

eccentricities of ellipses. The different ellipses created different types of movements; and both trajectory and velocity varied with the eccentricity of the ellipse.

Method

Subjects

35 Rice University undergraduates (27 female) participated for credit toward a course requirement. The participants had a mean age of 19.8 years (18-22). All subjects were right-handed.

Apparatus

Stimuli for the experiment were displayed on a Viewsonic VA503b 15" LCD monitor set at a resolution of 1024 x 768 pixels. Subjects were placed directly in front of the display and interacted using a Logitech M-UAE96 mouse. Mouse acceleration was turned off. Two identical Macintosh mini 1.83 GHz Intel Core 2 Duo machines running Mac OS X 10.6.8 were used for the experiment.

Stimuli and Design

During each trial a blue starting circle, contained between two ellipses drawn in black, was shown on the screen. A trial began when the mouse left the starting circle and ended when it returned. While the mouse was outside of the starting circle, the circle was shown as orange. The starting circle remained stationary on the screen for the duration of the trial. The diameter of the start circle was the same as the distance between the two ellipses. The white space between the two black ellipses was the pathway that the subjects had to move around. A representative trial is shown in Figure 9.

Four independent variables were manipulated: start position, distance between the ellipses, X diameter of the ellipse, and Y diameter of the ellipse.

Start position. Previous research on the spring-target it was hypothesized that there are directional effects for different starting positions.. To examine these effects the starting circle was in three different positions on the ellipse. The positions were 0°, 45°, and 90°, shown in Figure 10. Making an ellipse at the 45° starting position is similar to the movement that a low performer would make on the spring-target task

Distance between the ellipses. The distance between the ellipses should affect the velocity of the movement because it limits the amount of allowable error on the path. Therefore three different distances were used: 50 pixels, 75 pixels, and 100 pixels. For the analysis this measure is referred to as the path width.

X and Y Diameter. To create different eccentricities of the ellipse three different values for the X and Y Diameter were used. The three values used were 400, 550, and 700 pixels.

A full factorial design of the four independent variables was used resulting in 81 trials in each block. Two successful repetitions of each trial had to be performed resulting in 162 successful trials for each subject. The trials were presented in a random order in each block. Subjects completed five practice trials before the two task blocks to orient themselves to the task. The duration of the experiment was approximately one hour.

Procedure

At the beginning of a trial, the mouse automatically moved to the center of the starting circle. Subjects were instructed to move the mouse around the white elliptical path in a counter-clockwise direction without touching the black bounding lines until they returned to the starting circle. Figure 11 shows a trial in progress. Subjects were asked to not lift the mouse off the table unless they were about to move off the table. Subjects were allowed to lift the mouse when it was in the starting circle so that they could have an optimum starting position for the current

trial. If the subject touched the black outline of the ellipse or went outside the bounds with the mouse the trial was scored as unsuccessful. Subjects were not given any explicit feedback on whether they completed the trial successfully. When a trial was completed there was a five second pause and then the next trial appeared. If the trial was scored as unsuccessful the subject had to repeat the trial in a new block of trials at the end of the experiment.

A time stamped output of the mouse position was recorded throughout the task. All trials were presented in one session. Subjects were asked to fill out a short survey after completing the session. The survey contained questions about their computer use, experience, and questions eliciting their opinion on the experiment.

Results

Trajectory

The trajectories for all subjects on nine separate trials are shown in Figure 12. For these trials you can see that at the smallest path width many of the subjects used the same trajectory. As the path width increases the overlap in trajectories decrease. Independent of trials type the trajectories are made up of mostly straight-line sub movements around the path rather than a long curved movements. These straight-line movements become move pronounced on the oblong shapes where straight movements can be made for a longer period of time.

Mean Completion Time

A repeated measures ANOVA was run for experiment one to examine the effect of the independent measures on the completion time. The completion time for sixteen trials was replaced with the subject mean due to the subject not following directions on that trial.

The mean completion time for all trials in experiment one was 6550 milliseconds (ms) with a range from 920 ms to 33753 ms and a standard deviation of 417 ms.

Success Number. Since the subjects were required to complete each trial successfully twice the success number was assigned to the trial in the order it was completed successfully. The mean completion time for the two successes is shown in Figure 13. The main effect of success number on mean completion time is reliable ($F(1, 34) = 19.19$, $MSE = 51132137$, $p < .001$, $\eta^2_p = .36$). The subjects demonstrated a faster completion time on the second success than on the first success. This effect is likely caused by practice.

Start Position. Figure 14 shows the interaction between the start position and success number. The interaction is reliable ($F(2, 68) = 27.19$, $MSE = 3437721$, $p < .001$, $\eta^2_p = .55$). Two repeated measures ANOVAs separated by success number were run, the effect of start position on the first success if reliable, ($F(2, 68) = 34.45$ $MSE = 5265072$, $p < .001$, $\eta^2_p = .50$ Huyhn-Feldt adjustment) but on the second success the effect is no longer reliable ($F(2, 68) = 1.77$ $MSE = 263640$, $p = .179$, $\eta^2_p = .05$). The mean completion times for the three start positions are shown in Figure 15. The main effect of start position on completion time is reliable ($F(2, 68) = 16.05$, $MSE = 3283885$, $p < .001$, $\eta^2_p = .52$). A post-hoc custom contrast was run and when the start position is at 45 degrees, the time to complete the trial is reliably slower than at start positions 0 degrees and 90 degrees ($t(34) = -5.65$, $p < .001$, Scheffe adjustment). Three other two-way interactions with start position are significant but it is not clear what the sources of these effects are or what their meaning is. These interactions are start position and the X diameter, shown in Figure 16, ($F(4, 136) = 11.07$, $MSE = 2321955$, $p < .001$, $\eta^2_p = .53$), start position and Y diameter, shown in Figure 17, ($F(4, 136) = 22.36$, $MSE = 3328266$, $p < .001$, $\eta^2_p = .63$, Huyhn-Feldt adjustment), and start position and path width, shown in Figure 18. ($F(4, 136) = 8.30$, $MSE = 3892112$, $p < .001$, $\eta^2_p = .40$, Greenhouse-Geisser adjustment).

Path Width. Figure 19 shows the interaction between the path width and X diameter and Figure 20 shows the interaction between path width and Y diameter. The interaction between path width and the X diameter is significant ($F(4, 136) = 44.90$, $MSE = 10713160$, $p < .001$, $\eta^2_p = .75$, Greenhouse-Geisser adjustment,) as well as the interaction between path width and the Y diameter ($F(4, 136) = 75.30$, $MSE = 5301214$, $p < .001$, $\eta^2_p = .84$, Greenhouse-Geisser adjustment). The mean completion time for the three path widths are shown in Figure 21. The mean completion time differs significantly based on the path width of the trial ($F(2, 68) = 141.56$, $MSE = 226221225$, $p < .001$, $\eta^2_p = .84$, Greenhouse-Geisser adjustment). As the path width increases, the time it takes to complete the trial decreases. This result was expected because with a larger path width there is more room for the subject to move without touching the boundaries, allowing the subject to move at faster velocities.

Diameter. Figure 22 shows the completion time increasing as the X diameter does. Figure 23 shows the completion time increasing as the Y diameter does. Both of the main effects of X diameter and Y diameter on mean completion time are reliable ($F(2, 68) = 179.29$, $MSE = 21538428$, $p < .001$, $\eta^2_p = .87$, Greenhouse-Geisser adjustment; $F(2, 68) = 213.03$, $MSE = 21618376$, $p < .001$, $\eta^2_p = .88$, Greenhouse-Geisser adjustment). This result was expected due to it taking longer to complete a path as the length increases. The interaction between X and Y diameter is not reliable ($F(4, 136) = 2.40$, $MSE = 3072536$, $p = .073$, $\eta^2_p = .27$, Huyhn-Feldt adjustment). While the effect size of the Y diameter is a bit larger than the effect size of X diameter on completion time, Figure 24 shows that paired diameters have approximately the same completion time. Figure 25 shows the mean completion time for the X diameters across the two successes and Figure 26 shows the mean completion time for the Y diameters across the two successes. The mean completion time decreases from the first success to the second success

across all diameters. However the interaction between X diameter and success number is not significant ($F(2, 68) = 1.65$, $MSE = 3831017$, $p = .201$, $\eta^2_p = .07$); while there is a significant interaction between Y diameter and success number ($F(2, 68) = 13.48$, $MSE = 1945655$, $p < .001$, $\eta^2_p = .38$).

Other interactions. Table 1 shows the list of all three two-way and higher significant interactions for experiment one.

Errors

For experiment one, trials were considered unsuccessful if the mouse touched or went past the black bounding lines. Trials that were unsuccessful were classified as an error trial. In experiment one there were two ways that a subject could make an error. The first way is by touching or going outside the outer bounding circle. The second is by touching or going inside the inner bounding circle. Subjects repeated trials until they had been completed each trial successfully twice. The number of correct trials out of total trials usually defines error rate, since we did not use a fixed number of repetitions per trial this measure is not appropriate. The measure used here is the number of trials completed unsuccessfully before two were completed successfully. A repeated measure ANOVA was run to examine the effects of the independent variables on trial repetitions. No subjects or trials were excluded from the analysis.

There are a total of 1057 error trials. There was no difference in the number of error trials that were a result of moving outside the circle compared to inside the circle (50.24% to 49.76%). The mean number of error trials per subject is 30.4 with a standard deviation of 37.56 with the range from one to 146. The mean number of repetitions per for a trial before two correct trials is 0.373 with a range from 0.029 to 1.4 and a standard deviation of 0.350. For most trials the median number of repetitions is zero.

The mean number of repetitions for the three different path widths is shown in Figure 27. The path width has the largest impact on unsuccessful trials ($F(2, 68) = 23.43$, $MSE = 10.72$, $p < .001$, $\eta^2_p = .41$, Greenhouse-Geisser adjustment). A custom contrast comparing the path width of 50 pixels to the two larger path widths was run. When the path width is only 50 pixels it is more likely that the subject will make an error and have to repeat the trial ($t(34) = 4.51$, $p < .001$, Scheffe adjustment). The mean number of repetitions for the three X diameters is shown in Figure 28. The X diameter has a small effect on unsuccessful trials with more errors likely at longer diameters ($F(2, 68) = 7.86$, $MSE = 0.55$, $p = .001$, $\eta^2_p = .19$). There are also two significant interactions. The first is between path width and start position shown in Figure 29 ($F(4, 136) = 4.26$, $MSE = 0.72$, $p = .025$, $\eta^2_p = .11$). The second is between path width and X diameter shown in Figure 30 ($F(4, 136) = 3.12$, $MSE = 0.424$, $p = .032$, $\eta^2_p = .08$).

Steering Law Analysis

For the steering law analysis only successful trials were considered. Additionally trials were excluded if the subject did not make forward movements around the circle. The excluded trials were ones where the subject moved in and out of the starting circle without completely moving around the path or where the subject backtracked or made loops on their trajectory. There were 103 trials there were excluded from analysis leaving a total of 5567 trials. The excluded trials were not replaced.

For the steering law the index of difficulty is computed using the path length and the width of the path. In this experiment the width of the path was constant along the entire length of the path and equal to the distance between the two bounding ellipses. The path length was computed as the circumference of an imaginary ellipse that was half way between the two bounding ellipses minus the diameter of the starting circle. The diameter of the starting circle is

always the path width. This value was subtracted because data collection did not start until the subject left the circle and ended as soon as the subject returned to it. Since these values are constant across trials the index of difficulty is calculated using equation 7.

$$ID = \frac{2\pi\sqrt{(\frac{X^2_{diameter}+Y^2_{diameter}}{2})}-PathWidth}{PathWidth} \quad (7)$$

The model was tested with a linear regression run on individual subject's data. This method was used because if the regression were run across all subjects the individual differences between subjects' abilities to use the mouse would add noise to the model. The mean r^2 for the analysis is 0.67 with a range from 0.29 to 0.89 with a standard deviation of 0.166. The distribution of the r^2 values is shown in Figure 31. The individual r^2, *a*, and *b* values are shown in Table 2.

Due to the reliable effect of success number an additional linear regression analysis was run on the completion time data from success two. This analysis was also run as a fit on individual subjects. There were 2782 trials for this analysis. The mean r^2 for the linear models is 0.75 with a range from 0.41 to 0.88 and a standard deviation of 0.116. The distribution of the r^2 values is shown in Figure 32. The individual r^2, *a*, and *b* values are shown in Table 3.

Velocity Analysis

The same conditions that qualified a trial from exclusion from the Fitts's law analysis were used to exclude trials in the velocity analysis. Additionally only trials without a break in sampling were considered. The break in sampling was caused by an issue with the application that would pause data collection for up to 300 ms. With a sampling rate of approximately 0.1 ms this resulted in a large amount of missing data. A total of 4,983 trials were used in the analysis.

The rapid sampling rate also caused there to be many samples of the mouse in the same x,y position. Calculating the velocity directly from the data would result in the majority of the

samples having zero velocity with large spikes in velocity at the points where the mouse was moved. Since this is not an accurate representation of the mouse movement, a moving average was applied to smooth the velocity data. The window size that was used was 60 ms centered at the sample point. This window was selected due to previous experience in collecting data from the spring-target task.

2/3 Power Law. The common method to evaluate the motion data against the 2/3 Power Law is to calculate the curvature of movement at a given point on the users trajectory with Equation 6. The one-third root of the curvature is then correlated with tangential velocity at that point. The 2/3 power law did not correlate highly with the trajectories that the subjects produced. The mean r^2 across all subjects is 0.001 with a range from less than .0001 to .025. The per subject mean r^2 values with the range are shown in Table 4.

Minimum Jerk Analysis. For the analysis of the minimum jerk profile the algorithm that Todorov (1998) developed was used to construct the predicted profile. The aggregated path graphs were examined and it was found that the subjects on average produced nine segments that produced an octagon with the starting circle splitting one side. The input to the algorithm was the exit position of the starting circle, the eight vertices of the octagon located at the midpoint between the two bounding ellipses, the entrance to the starting circle, and the completion time of the trial. The algorithm output a time stamped trajectory, which the velocity was calculated from. The velocity of the subject at all samples was compared to the velocity of the prediction using r^2 and the mean absolute deviation. The mean r^2 was .015 with a range from .008 to .024. The mean absolute deviation across all trials was 0.436 with a range from 0.201 to 0.915. The per subject mean r^2, mean absolute deviation, and range of both measures are shown in Table 5.

The trial with the highest r^2 velocity was examined to gain some insight into the poor fit for the minimum jerk profile. Figure 33 shows the predicted velocity over the course of the trial and the actual velocity over the course of the trial. The predicted velocity shows an initial acceleration and then only small variations in velocity as it passes through the nine points of the octagonal path before making the final deceleration. The actual velocity plot shows many movements that start and stop as the subject makes movements around the path. While the r^2 value is the highest of any of the trials in the experiment this is mainly due to chance. This is because the minimum jerk profile predicts constant movement around the pathway and the subject's trajectory shows that they make many sub-movements as they navigate around the pathway.

EXPERIMENT TWO

The second experiment was designed to mirror the first experiment without the constraints of a bounded path. The levels and manipulation of the independent variables were the same across both experiments. A lot of the same effects that were in the first experiment were present in the second experiment but the unconstrained movement created other effects.

Method

Subjects

35 (29 female) Rice University undergraduates participated for credit toward a course requirement. The participants had a mean age of 19.5 (18-22). All subjects were right-handed and did not participate in the first experiment

Apparatus

Stimuli for the experiment were displayed on a Viewsonic VA503b 15" LCD monitor set at a resolution of 1024 x 768 pixels. Subjects were placed directly in front of the display and

interacted using a Logitech M-UAE96 mouse. Mouse acceleration was turned off. Two identical Macintosh mini 1.83 GHz Intel Core 2 Duo machines running Mac OS X 10.6.8 were used for the experiment.

Stimuli and Design

During each trial four items were displayed on the screen; the starting circle and three gateways. A representative trial is shown in Figure 34. The gateways are the black rectangles and the starting circle is shown in blue. A trial began when the mouse left the blue starting circle and ended when it returned. When the mouse was outside the starting circle it was orange. The starting circle and the gateways remained stationary on the screen during the trial. The diameter of the starting circle was the same as the size of the longest part of the gateway.

Four independent variables were manipulated: start position, gateway size, X diameter of the ellipse, and Y diameter of the ellipse.

Start position. To examine the effect of starting position on movement time the starting circle was in three different positions on the ellipse. The positions were 0°, 45°, and 90°. The different start positions are shown in Figure 35.

Gateway size. In this experiment the gateways were analogous to waypoints in previous experiments. This experiment manipulated the size of the gateway because it should affect the velocity of the movement. Therefore three different gateway sizes were used: 50 pixels, 75 pixels, and 100 pixels.

X and Y Diameter. To create different eccentricities of the ellipse three different values for the X and Y Diameter were used. The three values used are 400, 550, and 700 pixels. The outer edge of the gateway was positioned on the diameter of the bounding ellipse. The bounding ellipse was not visible to the subject.

A full factorial design of the four independent variables was used resulting in 81 trials in each block. Two repetitions of each trial were performed resulting in 162 trials presented to each subject. Trials that were not completed successfully were to be repeated in a new block at the end of the experiment. Due to an error in the programming of the experiment there were a variable number of correct trials for each subject. The trials were randomized in each block. At the beginning of the experiment, subjects completed five practice trials to orient themself to the task. The duration of the experiment was approximately half an hour.

Procedure

At the beginning of a trial the mouse was automatically moved to the center of the starting circle. Subjects were asked to leave the starting circle and move the mouse across each gateway and return to the circle. They were instructed to make the movement in a counter-clockwise direction around the screen. Figure 36 is an example of a trial in progress. When the mouse returned to the starting circle there was a five second pause and then the next trial would appear on the screen. If the mouse did not move across all of the gateways, the trial was scored as unsuccessful and they had to repeat it at the end of the block. Subjects were not given explicit feedback on whether the trials were completed successfully.

A time stamped output of the mouse position was recorded throughout the task. All trials were presented in one session. Subjects were asked to fill out a short survey after completing the session. The survey was the same as the one completed by the subjects in experiment one.

Results

Trajectory

The trajectories for all subjects on nine separate trials are shown in Figure 37. For these trials you can see that at the smallest gateway size many of the subjects used the same trajectory.

As the path width increases the overlap in trajectories decrease. For the start positions 0 and 90 degrees the subjects' movements are curved but at the 45 degrees start position the subjects make straight lines and hard turns at the gateways.

Mean Completion Time

For experiment two a repeated measures ANOVA was run to examine the effect of the independent measures on the completion time. Due to a recording error in experiment two, there were not 162 successful trials for each participant. For all participants the missing data were replaced with the subject mean. The total number of trials that were replaced with the mean is 398 out of 5670 trials (7%).

The mean completion time for all trials in experiment two is 2934 ms, with a range from 840 ms to 10548 ms and a standard deviation of 977 ms. Compared to the mean completion time for the trials in experiment one, the subjects in experiment two are faster. This is due to the removal of the boundary lines, which removes constraints on the subject's movement. The lack of bounds allows them to move at a higher velocity and take a shorter path to the gateway than moving between the boundaries would allow.

Success Number. The mean completion time for the two successes is shown in Figure 38. The main effect of success number on mean completion time is reliable ($F(1, 34) = 90.68$, $MSE = 262854774$, $p < .001$, $\eta^2_p = .73$). The subjects demonstrate a faster completion time on the second success than on the first success.

Start Position. Figure 39 shows the interaction between the start position and success number. This interaction is reliable ($F(2, 68) = 4.65$, $MSE = 697276$, $p = .013$, $\eta^2_p = .12$). In the second block, the effect of starting position disappears for start positions 0 degrees and 90 degrees, while at starting position 45 degrees the subjects take a shorter amount of time to

complete the task on both of the successes. The decrease between 0 degrees and 90 degrees is likely due to practice while the larger decrease in the 45 degrees condition is likely due to the subjects using a different strategy to complete the task. Two other two-way interactions with start position are significant but the source of their effect is not known. These interactions are start position and the X diameter, ($F(4, 136) = 18.08$, $MSE = 369215$, $p < .001$, $\eta^2_p = .35$, Figure 40, Huyhn-Feldt adjustment), and start position and Y diameter ($F(4, 136) = 23.41$, $MSE = 261903$, $p < .001$, $\eta^2_p = .41$, Figure 41). The mean completion times for the three start positions are shown in Figure 42. The mean completion time differs significantly across the different starting positions ($F(2, 68) = 7.63$, $MSE = 432540$, $p = .001$, $\eta^2_p = .18$). The completion time is the fastest at the 45 degrees start position and slowest at the 90 degrees start position.

Gateway Size. The interaction of success number and gateway size is reliable ($F(2, 68) = 15.27$, $MSE = 498762$, $p < .001$, $\eta^2_p = .31$, Huyhn-Feldt adjustment). Figure 43 shows that the completion time decreases from the first success to the second success. The mean completion time differed significantly across the gateway size for the trials ($F(2, 68) = 385.04$, $MSE = 1753352$, $p < .001$, $\eta^2_p = .92$, Huynh-Feldt adjustment). As the gateway size increases, the time it takes to complete the trial decreases. This result was expected because with a larger gateway size there is a greater area for the mouse to cross over, allowing the subject to travel at a higher velocity. The mean completion times for the three gateway sizes are shown in Figure 44.

Diameter. Figure 45 shows the completion time increasing as the X diameter does. Figure 46 shows the completion time increasing as the Y diameter does. Both of the main effects of X diameter and Y diameter on mean completion time are reliable ($F(2, 68) = 365.27$, $MSE = 714088$, $p < .001$, $\eta^2_p = .92$, Greenhouse-Geisser adjustment; $F(2, 68) = 386.42$, $MSE = 536951$, $p < .001$, $\eta^2_p = .92$, Huynh-Feldt adjustment). This result was expected due to it taking longer to

complete the movement around a path as the length increases. The interaction between X and Y diameter is reliable ($F(4, 136) = 6.35$, $MSE = 296095$, $p < .001$, $\eta^2_p = .16$, Huyhn-Feldt adjustment). Figure 47 shows that paired diameters have approximately the same completion time. The mean completion time decreases from the first success to the second one across all diameters (Figure 48 and Figure 49). The interaction between X diameter and success number is significant ($F(2, 68) = 18.47$, $MSE = 415206$, $p < .001$, $\eta^2_p = .35$, Huyhn-Feldt adjustment); as well as the interaction between Y diameter and success number ($F(2, 68) = 19.19$, $MSE = 279283$, $p < .001$, $\eta^2_p = .36$). The interaction between gateway size and the X diameter is significant and shown in Figure 50 ($F(4, 136) = 6.08$, $MSE = 440907$, $p < .001$, $\eta^2_p = .15$, Huyhn-Feldt adjustment). The interaction between path width and the Y diameter is also significant and shown in Figure 51 ($F(4, 136) = 4.06$, $MSE = 214285$, $p = .004$, $\eta^2_p = .11$,).

Other interactions. Table 6 shows the list of all three-way and higher significant interactions for experiment two.

Errors

Due to an error in the code subjects were only forced to repeat trials if they missed the first gateway. There were two other factors that caused subjects to repeat trials that were completed successfully. The first of these is that the program would stop collecting data to run garbage collection. The second is that the subjects' velocity was high enough that on the smaller gateways the subject could move across it so fast that no sample was registered on it. Due to the program errors, the experimenter evaluated each trial's trajectory to determine whether the trial was completed successfully. These three errors also led to an uneven number of trials for each subject and it was not guaranteed that there would be two successful trials for each subject. As a result a different error rate metric was used for this study. The error rate was the total number of

failures divided by the total number of times the trial was done before two successes were reached. A repeated measures ANOVA was run to examine the effects of the independent variables on the proportion of error trials.

For experiment two, trials were considered unsuccessful if the mouse did not cross all three gateways. Trials that were completed unsuccessfully were classified as error trials. There are a total of 663 error trials. Four types of errors were classified. The first type of errors is the subject returning to the starting circle after traveling a short distance, which accounted for 5.7% of the errors. The second type of error was due to recording problems, these accounted for 14.5% of the error trials. The other two sources of error are the same as the first experiment with 48.7% of error trials coming from the subject going inside of the gateways and 30.9% of the errors coming from the subjects going outside the gateways. The mean proportion of incorrect trials was 0.9 with a range from 0 to1 and a standard deviation of 0.21.

The independent variable that has the largest impact on unsuccessful trials is the gateway size ($F(2, 68) = 36.14$, $MSE = .04$, $p < .001$, $\eta^2_p = .52$). The error proportions for the three gateways are shown in Figure 53. When the gateway size is 50 the majority of the errors are committed. The error proportions for the three start positions are shown in Figure 52. The start position has a small effect on error rate with errors being less likely to occur at the 45 degrees start position. ($F(2, 68) = 3.79$, $MSE = .05$, $p = .028$, $\eta^2_p = .10$). The X diameter also has a small effect on unsuccessful trials with more errors likely at longer diameters ($F(2, 68) = 4.05$, $MSE = .036$, $p = .022$, $\eta^2_p = .11$). The error proportions for the three X diameters are shown in Figure 54.

Fitts's Law Analysis

For the Fitts's law analysis only the first two successful trials were used. Since Fitts's Law models aimed movement trials were excluded if the subject did not move from gateway to

gateway. An example trial is if the subject circled back to a gate if they thought the missed it. Also trials that veered very far off course were not considered in the analysis. A total of 5060 trials were used in the analysis.

This analysis utilized the Shannon formulation of Fitts's Law shown in Equation 8. This formulation has the advantage that it does not produce a negative index of difficulty giving a better fit than the original formulation. The amplitude for each movement was the distance from the center of one gateway to the next. For the amplitude of the first and second movement the radius of the starting circle was subtracted due to the fact the task did not start recording until the mouse left the circle. Three different metrics were compared for the width of the gateways. These metrics were the smaller side of the gateway (*smaller-of*), the larger side of the gateway (*larger-of*), and the width along the angle of approach (*w'*). MacKenzie and Buxton (1994) compared these models and found little difference between *smaller-of* and *w'*. This task differed due to the fact that the subjects had to move through three targets before stopping on the fourth where in MacKenzie and Buxton's task the subject only needed to hit one target. The starting circle's *W* was the diameter for all three conditions.

$$MT = a + b\log_2(\frac{A}{w} + 1) \quad (8)$$

A least squares linear regression model was fit to the movement time data for individual subjects to control for individual differences. The distributions of the r^2 values for all three indices of difficulty are shown in Figure 55. The individual r^2, a, and b values are shown in Table 7. The mean r^2 for the *smaller-of* model is 0.52 with a range from 0.20 to 0.78 with a standard deviation of 0.121. The *larger-of* model produced a similar result; the mean is 0.52 with a range from 0.20 to 0.78 and a standard deviation of 0.122. The *w'* model produced worse results with a mean of 0.49 a range from 0.19 to 0.73 and a standard deviation of 0.112.

Since the second success was significantly faster than the first success an additional analysis was run on the second successful trials. There were a total of 2397 trials used in this analysis. The distributions of the r^2 values for all three indices of difficulty are shown in Figure 56. The individual r^2, *a*, and *b* values are shown in Table 8. The mean r^2 for the *smaller-of* model is 0.63 with a range from 0.10 to 0.82 with a standard deviation of 0.152. The *larger-of* model produced a similar result; the mean is 0.63 with a range from 0.10 to 0.82 and a standard deviation of 0.155. The *w'* model produced worse results with a mean of 0.59 a range from 0.10 to 0.76 and a standard deviation of 0.144.

Velocity Analysis

The same conditions that qualified a trial from exclusion from the Fitts's law analysis excluded trials in the velocity analysis. The same sampling interruption issue occurred in experiment two causing trials with large breaks in recording to be excluded from analysis. For the analysis 4839 trials were used. Additionally the same moving average function that was utilized in experiment one was used to smooth the data in experiment two.

2/3 Power Law. The same method used in experiment one to analyze the trajectory against the 2/3-power law was also used to analyze the data in this experiment. The 2/3-power law did not correlate highly with the trajectories that the subjects produced. The mean r^2 across all subjects is .0005 with a range from less than .0001 to .022. The per subject mean r^2 values with the range are shown in Table 9.

Minimum Jerk Analysis. For the analysis of the minimum jerk profile the algorithm that Todorov (1998) developed was used to construct the predicted profile. The input to the algorithm was the exit position of the starting circle, the center of the three gateways, the entrance to the starting circle, and the completion time of the trial. The algorithm output a time stamped

trajectory, which the velocity was calculated from. The velocity of the subject at all samples was compared to the velocity of the prediction using r^2 and the mean absolute deviation. The mean r^2 was .013 with a range from .006 to .018. The mean absolute deviation across all trials was 0.721 with a range from 0.401 to 1.140. The per subject mean r^2, mean absolute deviation, and range of both measures are shown in Table 10.

The trial with the highest r^2 velocity was examined to gain some insight into the poor fit for the minimum jerk profile. Figure 57 shows the predicted velocity over the course of the trial and the actual velocity over the course of the trial. The predicted velocity shows an initial acceleration and then only small variations in velocity as it passes through the four gateways before making the final deceleration. The actual velocity plot shows many movements that start and stop as the subject makes movements around the path. While the r^2 value is the highest of any of the trials in the experiment this is mainly due to chance. This is because the minimum jerk profile predicts constant movement around the pathway and the subject's trajectory shows that they make many sub movements as they navigate around the pathway.

Discussion

The expected effects of many of the independent variables on completion time were evident in this experiment. Fitts's law and its derivation the Steering law predict that the longer the path length the more time it takes to move along a path. These laws also predict that as the target size or path size decrease the movement time will take longer. The subjects' movement times are in line with this theory. The longer the pathway the more time it took to complete the trial and as the path width and gateway size decreased the completion time increased. The error rate was also related to these metrics. The longer path lengths and smaller path widths or gateway sizes had larger error rates. This is due to the fact that for longer path widths there is

more of a chance to make an error. For the smaller path widths and gateway sizes there is a smaller target space so there is a greater likelihood that the subjects will make an error. This is also evident when examining the trajectories. At the smaller path widths the subjects' trajectories have greater overlap than at the larger path widths. A related result is, the completion time for experiment two was much shorter than the completion time for experiment one. This is due to the fact that the majority of the movement was unbounded. The only parts of the movement that were constrained were when the subjects passed through the gateways. For the bounded ellipse experiment the steering law showed higher predictive power than Fitts's Law did for the less constrained motion experiment. This was likely due to the subjects' motion being constrained to a more predictable pathway. While the subjects were instructed to move from gateway to gateway during the second experiment, where they changed directions in their trajectory was not always at the gateway. Even considering this fact the set of trials that were analyzed were ones where their general movement was not off track from gateway to gateway. The low predictive power of Fitts's Law in this situation was unexpected. The performance improvement in completion time from the first success to the second success was not anticipated. While the task was different from everyday computer usage it was expected that subjects would be well practiced with moving the mouse around the screen, as it is a common task.

There were some other unexpected effects. One of these was that the subjects clearly made sub-movements around the pathway rather than a continuous movement. This work set out to examine the predictive power of the current models on a continuous curved path. This was not the behavior that the subjects displayed, and the possible causes of it will be discussed in more detail later. Another interesting effect that emerged was from trials in the first experiment that had the 45 degrees start position. Subjects in the first experiment were initially slower when

moving from this position. However this behavior was not consistent across successes and disappeared on the second one. There were also a number of significant interactions with start position, the sources of which are still unknown. The 45-degree start position also had interesting effects in the second experiment. With just the visual cues changed, the trajectories changed drastically with harder turns and straighter movements between gateways. This allowed the subjects to complete the trials faster than when the start positions were at 0 and 90 degrees. Another unexpected effect was that of the X diameter on the error rate. This could be caused by a number of issues. Since the interaction with X diameter and start position was reliable the source of this effect could be due to repositioning the mouse between trials. Another source of this effect could be that the horizontal movement is harder at longer axis lengths because the movement could cause the subject to extend their arm past the midline of the plane of movement.

One aspect of the data analysis that could be examined is the velocity-smoothing method. It may be that size of the moving average window used for the velocity smoothing function may not have been large enough. While the size was determined based on previous research, this experiment may have needed a different sized window. There are problems associated with making the window too large. One major problem is that as the window length increases, it obscures the length of pause points and if it is too large it will get rid of them entirely. This experiment had definite pause points due to the sub-movements that subjects made. The best smoothing function is not something that is defined in the literature and different experimenters utilize different ones.

While this work set out to see which theory explained more of the variance in the velocity profiles, there was little evidence that either of the theories had predictive power in this experiment. In previous work the 2/3 power law explained a significant amount of the variance

of the movement. In this experiment the subjects' movements were not curved but linear so the theory did not apply. The majority of the times the subjects made a change in direction, which would produce larger instantaneous curve values, were after they started moving from a pause point. While the theory states that at a large curve the subject will slow down it does not predict that they will stop. In the case of the minimum jerk profile, even if the pause points were obscured with a smoothing technique the velocity profiles still would not match. The minimum jerk profile predicts that the velocity graphs will make a bell shaped pattern with small deviations based on waypoints the subject passes through. This is due to the fact that the profile predicts a single continuous movement. In this experiment the subjects made a series of sub-movements with short pauses between the movements as they completed the path.

One of the reasons that this experiment may have generated a different type of movement is the length of the path. Previous experiments have given the subjects an explicit shape to draw. Especially with research into the 2/3 power law it is common to give the subjects a path and the instruction to trace the pathway continuously for some amount of time. Deviations from the drawn path are not counted as errors as the researchers are more concerned with the velocity of the movement than with the path. With research into the minimum jerk profile it is common for subjects to be presented with a single point to move toward and even when they were given multiple points the path lengths were smaller than the ones used in this experiment. If the trials in this work contained paths with more variation in their length it might be possible to discover at what size subjects stop making continuous movements and start to make different types of movements. This work also varied from past work in the instructions that were given to the subjects. Specifically in relation to the minimum jerk profile, subjects in Todorov's experiment were told to connect the points in by making a curve. Subjects in these experiments were

allowed to plan their own trajectories as long as their movement met the constraints to not be an error trial.

Future work could explore over what path lengths subjects movement is explained by the minimum jerk profile and figure out the boundary where the minimum jerk profile no longer represents the velocity profile. Another direction that the work could take would be to present the larger path lengths in a manner that is similar to past work. In the second experiment the 45 degrees condition was visually different enough to change the type of movement that the subjects made. Todorov and Jordan (1998) instructed the subjects to move through specific points, as opposed to gateways, and varied the number and pattern of points presented to the subjects. Work by Viviani and colleagues presented the subjects with explicit paths to trace but did not require the movement to remain on the path. It is possible that this work would have found different results if the path lengths and eccentricities were the same but the visual presentations of the trials were similar to past work. The visual presentation of the task could have a large effect on the type of movement that the subjects generate.

To be able to implement a cognitive model that could do the first experiment there would have to be a number of extensions made to ACT-R. While the Steering law could be used to predict the time on a subject-to-subject basis, more information is required to compute the trajectory and velocity. The first extension needed would be a predictive model of the location of the pause points between movements. While the data collected in this experiment could aid in this, a number of other sources could add valuable information. Predicting sub movements could be similar to predicting sub goals, as there are efficiency and energy considerations. It would also be interesting to compare the sub-movements made by the motor system to the scanning and fixation patterns of the eye to see if there are any similarities. Once a model of the pause points is

implemented the data from this experiment could aid in determining the velocity profile between pause points. The model that may explain the movement could be a variation of the minimum jerk profile where the individual movements between pause points match the velocity profile but a full stop is made between movements. This does not have to be the case as there are other velocity profiles like the minimum snap and minimum crackle. It is also unlikely that the minimum jerk profile is used, as the peak velocities are higher than the ones predicted by the model.

Implementing a cognitive model of the second experiment provides similar as well as unique challenges to implementing the first. One of the major challenges is that there is not a confined path in this experiment. This creates a much larger space for the pause points to be in. If the pause points were the gateways then Fitts's law would have a higher predictive power than is evident in this experiment. If a predictive model of the sub-movements is generated, Fitts's law could be applied to the movement between those points and it may provide more predictive power. Similar to the first experiment once the sub movements are predicted the velocity profile that predicts the trajectory and velocity between them could be generated from the data in this experiment. What that velocity profile best predicts is again an open question.

While this work set out to model curved movement in two specific tasks, it instead generated different results. These tasks are ones that the existing models do not support. Additional research, specifically into the area of predicting sub movements of a larger movement, is needed before a cognitive model can be implemented. Future work could further address at what point the theories no longer apply and the movement changes from a continuous one to one made up of smaller ones.

Reference

Accot, J., & Zhai, S. (1997). Beyond Fitts' Law: Models for trajectory-based HCI tasks. *CHI '97 Proceedings of the SIGCHI conference on Human factors in computing systems,* 295-392.

Anderson, J. R. (2007). *How can the human mind occur in the physical universe?* New York: Oxford University Press.

Byrne, M. D., O'Malley, M. K., Gallagher, M. A., Purkayastha, S. H., Howie, N., & Huegel, J. C. (2010). A Preliminary ACT-R model of a continuous motor task. *In Proceedings of the Human Factors and Ergonomics Society 53nd Annual Meeting,* 1037-1041.

Fitts, P.M. (1954). *The teaching of handwriting*. Boston: Houston Mifflin.

Flash, T., & Hogan, N. (1985). The coordination of arm movements: an experimentally confirmed mathematical model. *Journal of Neuroscience,* 5, 1688-1703.

Hogan, N. (1984). An organizing principle for a class of voluntary movements. *Journal of Neuroscience*, 4, 2745–2754.

Huegel, J. (2009). *Progressive Haptic Guidance for a Dynamic Task in a Virtual Training Environment.* Doctoral Dissertation, Rice University, Houston, TX.

Huegel, J., Celik, O., Israr, A., & O'Malley, M. K. (2009). Expertise- based performance measures in a virtual training environment. *Presence: Teleoperators and Virtual Environments*, *18*(6), 449– 467.

Jagacinski, R. J., & Flach, J. M. (2003). *Control theory for humans: Quantitative approaches to modeling performance*. Mahwah, NJ: Erlbaum.

Lacquanti, F., Terzuolo, C., & Viviani, P. (1983). The law relating kinematics and figural aspects of drawing movements. *Acta Psychology* 54, 115-130.

Lank, E., Saund, E., & May, L. (2005). Sloppy selection: Providing an accurate interpretation of imprecise selection gestures. *Computers & Graphics,* 4, 490-500.

Li, Y., Huegel, J., Patoglu, V., & O'Malley, M. K. (2009). Progressive shared control for training in virtual environments. *In Proceedings of the International Symposium on Haptic Interfaces for Virtual Environment and Teleoperator Systems and the Third Joint World Haptics Conference (HAPTICS*), 332–339.

Li, Y., Patoglu, V., & O'Malley, M. K. (2009). Negative efficacy of fixed gain error reducing shared control for training in virtual environments. *ACM Transactions on Applied Perception*, 6, 1–21.

Mackenzie, I. S. (1992). Fitts' Law as a research and Design tool in human-computer interaction. *Human Computer Interaction*, 7, 91-139.

MacKenzie, I. S., & Buxton, W. (1992). Extending Fitts' law to two-dimensional tasks. *Proceedings of the ACM Conference on Human Factors in Computing Systems - CHI '92*, 219-226.

O'Malley, M. K., Gupta, A., Gen, M., & Li, Y. (2006). Shared control in haptic systems for performance enhancement and training. *ASME Journal of Dynamic Systems, Measurement and Control,* 128, 75–85.

Richardson, M. J. E. & Flash, T. (2002). Comparing smooth arm movements with the two-thirds power law and the related segmented-control hypothesis. *The Journal of Neuroscience, 22*(18), 8201-8221.

Todorov, E. & Jordan, M. I. (1998). Smoothness maximization along a predefined path accurately predicts the speed profiles of complex arm movements. *Journal Neurophysiology*, *80*(2), 696-714.

Viviani, P., & Terzuolo, C. (1982). Trajectory determines movement dynamics.

Neuroscience, 7:431-437

Table 1.

Results of higher order interactions from Repeated Measures ANOVA on the completion time in experiment one

Within Subject Effect		*p*	Correction	η^2_p
Start Position * X Diameter * Y Diameter	F(8, 272) = 4.82	< .001	Huyhn-Feldt	.12
Start Position * Y Diameter* Path Width	F(8, 272) = 18.92	< .001	Greenhouse-Geisser	.36
Start Position * Y Diameter * Success Number	F(4, 136) = 15.04	< .001		.31
Start Position * Path Width * Success Number	F(4, 136) = 7.53	< .001		.18
X Diameter * Y Diameter * Path Width	F(8, 272) = 10.41	< .001	Greenhouse-Geisser	.23
X Diameter * Y Diameter * Success Number	F(4, 136) = 3.90	.009	Huyhn-Feldt	.10
X Diameter * Path Width *Success Number	F(4, 136) = 9.62	<.001	Huyhn-Feldt	.22
Y Diameter * Path Width *Success Number	F(4, 136) = 10.41	< .001		.23
Start Position * X Diameter * Y Diameter * Path Width	F(16, 544) = 13.03	< .001	Greenhouse-Geisser	.28
Start Position * X Diameter	F(8, 272) = 10.72	< .001	Greenhouse-Geisser	.24

* Y Diameter * Success Number				
Start Position * X Diameter * Path Width * Success Number	F(8, 272) = 2.96	= .008	Huyhn-Feldt	.08
Start Position * Y Diameter * Path Width * Success Number	F(8, 272) = 5.93	< .001	Greenhouse-Geisser	.15
X Diameter * Y Diameter * Path Width * Success Number	F(8, 272) = 19.57	< .001	Huyhn-Feldt	.37
Start Position * X Diameter * Y Diameter * Path Width * Success Number	F(16, 544) = 7.88	< .001	Greenhouse-Geisser	.20

Table 2.

Results of the regression of Index of difficulty on completion time for both successes in experiment one.

Subject	Intercept	Slope	r^2
s3	-1687.93	516.16	0.844
s4	-166.03	256.8	0.747
s5	882.2	210.37	0.582
s6	-61.31	454.02	0.695
s7	-601.4	617.97	0.838
s8	-1167.7	544.32	0.793
s9	931.5	122.27	0.291
s10	1537.74	139.31	0.322
s11	-1367.77	643.71	0.820
s12	-445.24	412.37	0.589
s13	1430.21	220.53	0.650
s14	946.39	309.79	0.718
s15	-122.63	308.64	0.815
s16	1196.06	235.3	0.363
s17	881.03	320.73	0.751
s18	715.99	416.96	0.745
s19	-1717.41	534.18	0.853
s20	553.3	254.63	0.781
s21	1121.32	206.26	0.694

s22	119.69	328.59	0.815
s23	330.6	286.44	0.747
s24	341.19	245.4	0.731
s25	995.2	156.1	0.376
s26	-880.93	416.39	0.689
s27	1357.54	240.23	0.571
s28	164.521	280.787	0.846
s29	-401.48	340.75	0.799
s30	1535.943	133.467	0.709
s31	-101	408.81	0.689
s32	-392.82	518.08	0.724
s33	-719.57	521.89	0.893
s34	1029.61	215.24	0.417
s35	1364.23	107.25	0.465
s36	1156.46	189.3	0.654
s37	676	291.5	0.467

Table 3.

Results of the regression of index of difficulty on completion time for the second success in experiment one.

Subject	Intercept	Slope	r^2
s3	-1817.64	504.78	0.875
s4	-198.99	267.54	0.838
s5	833.47	180.15	0.772
s6	412.64	383.84	0.760
s7	-785.54	602.57	0.882
s8	-949.72	522.64	0.819
s9	901.894	77.842	0.565
s10	1285.77	117.95	0.506
s11	-1533.13	657.79	0.844
s12	-336.16	331.76	0.796
s13	282.92	256.96	0.840
s14	493.02	307.86	0.722
s15	-390.83	314.04	0.837
s16	1029.58	170.49	0.704
s17	592.52	371.89	0.815
s18	346.5	403.7	0.782
s19	-2057.67	576.52	0.870
s20	638.15	247.18	0.733
s21	893.44	200.68	0.772

s22	179.36	318.53	0.830
s23	-3.275	325.603	0.764
s24	-16.75	275.46	0.746
s25	1137.99	131.15	0.411
s26	75.6	327.2	0.697
s27	707.26	236.13	0.760
s28	256.56	269.8	0.856
s29	-701.7	340.8	0.811
s30	1419.138	127.567	0.803
s31	-358.09	441.63	0.723
s32	282.77	408.7	0.791
s33	-446.73	512.04	0.884
s34	1219.8	144.77	0.721
s35	589.72	149.43	0.568
s36	1214.77	162.8	0.718
s37	1269.2	243	0.485

Table 4.

Results of the correlation of tangential velocity and the one-third root of curvature per subject for experiment one.

Subject	Mean r^2	Minimum	Maximum
s3	0.0012	0.0000	0.0094
s4	0.0016	0.0000	0.0154
s5	0.0013	0.0000	0.0153
s6	0.0016	0.0000	0.0187
s7	0.0013	0.0000	0.0157
s8	0.0014	0.0000	0.0149
s9	0.0014	0.0000	0.0208
s10	0.0015	0.0000	0.0240
s11	0.0013	0.0000	0.0138
s12	0.0017	0.0000	0.0243
s13	0.0014	0.0000	0.0108
s14	0.0017	0.0000	0.0108
s15	0.0015	0.0000	0.0174
s16	0.0019	0.0000	0.0188
s17	0.0015	0.0000	0.0151
s18	0.0017	0.0000	0.0156
s19	0.0013	0.0000	0.0153
s20	0.0015	0.0000	0.0179
s21	0.0014	0.0000	0.0186

s22	0.0012	0.0000	0.0142
s23	0.0017	0.0000	0.0181
s24	0.0015	0.0000	0.0246
s25	0.0010	0.0000	0.0184
s26	0.0014	0.0000	0.0125
s27	0.0020	0.0000	0.0234
s28	0.0015	0.0000	0.0168
s29	0.0015	0.0000	0.0183
s30	0.0010	0.0000	0.0128
s31	0.0017	0.0000	0.0207
s32	0.0016	0.0000	0.0151
s33	0.0013	0.0000	0.0155
s34	0.0019	0.0000	0.0168
s35	0.0007	0.0000	0.0083
s36	0.0011	0.0000	0.0089
s37	0.0017	0.0000	0.0245

Table 5.

Results of the correlation of experimental velocity and the predicted minimum jerk velocity and the mean absolute deviation of the experimental velocity from the predicted minimum jerk velocity for experiment one.

Subject	Mean r^2	Minimum	Maximum	Mean Absolute Deviation	Minimum	Maximum
s3	0.0145	0.0097	0.0193	0.2082	0.0822	0.4067
s4	0.0148	0.0101	0.0197	0.3047	0.1176	0.6087
s5	0.0150	0.0095	0.0195	0.2879	0.0966	0.5553
s6	0.0157	0.0102	0.0232	0.1730	0.0538	0.3318
s7	0.0161	0.0102	0.0208	0.1365	0.0504	0.2352
s8	0.0162	0.0122	0.0216	0.1645	0.0613	0.2945
s9	0.0141	0.0098	0.0197	0.4358	0.1228	0.9147
s10	0.0146	0.0106	0.0206	0.3359	0.1084	0.5761
s11	0.0162	0.0103	0.0221	0.1471	0.0546	0.2700
s12	0.0169	0.0123	0.0218	0.2011	0.0598	0.4431
s13	0.0151	0.0093	0.0188	0.2477	0.1108	0.4496
s14	0.0153	0.0093	0.0210	0.2108	0.0921	0.3498
s15	0.0158	0.0109	0.0204	0.2507	0.1160	0.4213
s16	0.0155	0.0103	0.0217	0.2557	0.0820	0.4542
s17	0.0160	0.0119	0.0222	0.1994	0.1041	0.3477
s18	0.0162	0.0109	0.0224	0.1655	0.0666	0.2808
s19	0.0167	0.0115	0.0226	0.1884	0.0657	0.3756

s20	0.0157	0.0113	0.0212	0.2523	0.1277	0.4282
s21	0.0148	0.0102	0.0187	0.2725	0.1355	0.4375
s22	0.0153	0.0113	0.0195	0.2235	0.1014	0.4337
s23	0.0164	0.0120	0.0218	0.2380	0.0959	0.4096
s24	0.0150	0.0105	0.0200	0.2809	0.1160	0.5049
s25	0.0147	0.0103	0.0197	0.3540	0.1178	0.6586
s26	0.0152	0.0077	0.0208	0.2321	0.0654	0.4745
s27	0.0155	0.0102	0.0198	0.2384	0.0879	0.4263
s28	0.0156	0.0094	0.0203	0.2513	0.1196	0.4062
s29	0.0150	0.0108	0.0202	0.2446	0.0943	0.4222
s30	0.0149	0.0096	0.0183	0.3120	0.1783	0.5002
s31	0.0155	0.0111	0.0204	0.1935	0.0731	0.3897
s32	0.0156	0.0080	0.0237	0.1652	0.0660	0.3125
s33	0.0159	0.0116	0.0218	0.1659	0.0809	0.2855
s34	0.0159	0.0108	0.0216	0.2674	0.0922	0.4715
s35	0.0140	0.0101	0.0174	0.3971	0.2014	0.7193
s36	0.0147	0.0096	0.0205	0.2925	0.1456	0.5256
s37	0.0159	0.0113	0.0207	0.2423	0.0747	0.4366

Table 6.

Results of higher order interactions from Repeated Measures ANOVA on the completion time in experiment 2

Within Subject Effect		*p*	Correction	η^2_p
Start Position * X Diameter * Y Diameter	F(8, 272) = 2.12	.034		.06
Start Position * X Diameter * Success Number	F(4, 136) = 7.12	< .001		.17
Start Position * Y Diameter* Path Width	F(8, 272) = 8.61	< .001	Greenhouse-Geisser	.19
Start Position * Y Diameter * Success Number	F(4, 136) = 8.35	< .001		.20
X Diameter * Y Diameter *Success Number	F(8, 272) = 4.11	< .001	Huyhn-Feldt	.11
X Diameter * Path Width *Success Number	F(4, 136) = 13.51	< .001	Greenhouse-Geisser	.28
Start Position * X Diameter * Y Diameter * Path Width	F(16, 544) = 7.63	< .001	Greenhouse-Geisser	.18
Start Position * X Diameter * Y Diameter *	F(8, 272) = 6.06	< .001	Greenhouse-Geisser	.15

Success Number				
Start Position * Y Diameter * Path Width * Success Number	F(8, 272) = 5.71	< .001	Greenhouse-Geisser	.14
X Diameter * Y Diameter * Path Width * Success Number	F(8, 272) = 6.52	< .001	Greenhouse-Geisser	.16
Start Position * X Diameter * Y Diameter * Path Width * Success Number	F(16, 544) = 5.88	< .001	Greenhouse-Geisser	.15

Table 7.

Results of the regression of index of difficulty on completion time in experiment 2.

	Larger			Smaller			W'		
Subject	a	b	r^2	a	b	r^2	a	b	r^2
s1	601.51	205.46	0.391	-272.58	180.02	0.394	20.81	177.58	0.382
s2	584.52	262.01	0.613	-514.72	228.52	0.609	-81.08	221.32	0.571
s3	-37.05	457.22	0.276	-1922	396.57	0.272	-1311.59	394.22	0.271
s4	543.41	269.9	0.585	-598.66	236.03	0.584	-132.97	227.41	0.548
s5	324.48	318.29	0.608	-995.72	276.65	0.603	-412.6	263.9	0.554
s6	153.5	235.8	0.656	-823.3	204.85	0.649	-381.5	194.45	0.593
s7	63.87	298.56	0.532	-1180.88	259.93	0.529	-647.92	249.09	0.490
s8	366.4	256.83	0.607	-705.48	223.67	0.605	-234.18	212.99	0.553
s9	498.86	296.58	0.781	-752.1	259.1	0.778	-250.23	250.34	0.726
s10	297.39	218.78	0.566	-621	190.85	0.563	-259.6	184.88	0.520
s11	328.88	289.38	0.636	-885.18	252.39	0.633	-390.53	243.31	0.5915
s12	831	251.9	0.581	-230.32	219.98	0.579	264.47	207.7	0.5147
s13	1069.76	250.3	0.201	20.23	218.26	0.200	408.79	213.05	0.1915
s14	211.64	247.89	0.651	-827.8	216.17	0.651	-490.77	214.05	0.6273
s15	750.02	181.55	0.541	1.72	157.5	0.532	284.91	153.91	0.5131
s16	100.2	334	0.474	-1285.39	290.28	0.471	-689.34	277.87	0.4291
s17	918.65	171.77	0.428	189.7	150.34	0.429	428.25	148.79	0.4203
s18	192.23	259.49	0.528	-885.02	225.61	0.516	-448.47	217.9	0.4836
s19	-44.6	232.94	0.694	-1019.65	203.01	0.688	-637.7	197.2	0.6427

s20	294.98	289.38	0.610	-917.58	252.3	0.608	-486.8	247.8	0.588
s21	665.04	253.29	0.514	-382.34	219.95	0.508	79.34	209.87	0.4657
s22	427.62	359.95	0.504	-1075.12	313.46	0.500	-448.61	301.44	0.4647
s23	-615.93	416.36	0.616	-2352.42	362.51	0.610	-1592.98	346.03	0.5589
s24	770.1	287.17	0.515	-433.54	250.39	0.510	16.95	243.86	0.4859
s25	-176.1	355.67	0.360	-1655.16	309.45	0.355	-1175.94	306.54	0.3504
s26	847.18	240.35	0.440	-165.81	209.95	0.439	208.31	204.92	0.4153
s27	819.98	271.14	0.572	-315.51	236.35	0.568	56.87	234.53	0.5566
s28	122.43	225.85	0.559	-822.41	196.81	0.556	-482.38	193.24	0.5359
s29	71.3	270.36	0.455	-1061.73	235.7	0.452	-589.23	226.14	0.4269
s30	442.59	250.72	0.422	-600.5	218.2	0.418	-218.73	213.62	0.4002
s31	302.84	156.33	0.566	-343.77	135.77	0.561	-75.53	130.66	0.5134
s32	32.84	356.18	0.452	-1458.72	310.52	0.450	-766.21	293.63	0.4067
s33	771.86	204.88	0.279	-109.59	180.11	0.285	273.86	171.41	0.2549
s34	79.65	269.02	0.582	-1053.32	234.89	0.583	-671.89	232.37	0.5573
s35	150.41	230.86	0.508	-823.8	201.8	0.506	-434.31	195.15	0.4728

Table 8.

Results of the regression of index of difficulty on completion time for the second success in experiment 2.

	Larger			Smaller			w'		
Subject	a	b	r2	a	b	r2	a	b	r2
s1	468.31	198.18	0.5686	-375.23	173.73	0.5711	-33.54	167.18	0.5307
s2	254.59	271.8	0.7318	-883.32	236.89	0.7255	-430.68	229.16	0.6761
s3	788.58	281.59	0.3225	-398.55	245.92	0.3245	113.93	234.79	0.2979
s4	682.9	233.31	0.6167	-307.66	204.23	0.6169	69.1	198.69	0.5916
s5	204.54	299.72	0.7369	-1035.5	260.3	0.7328	-480.22	247.53	0.6772
s6	63.53	236.12	0.6807	-905.25	204.49	0.6718	-479.58	194.94	0.6267
s7	355.44	235.28	0.7525	-633.88	205.38	0.7544	-229.39	198.1	0.7124
s8	293.63	258.49	0.6739	-774.02	224.35	0.6656	-328.19	215.6	0.6229
s9	351.07	314.62	0.7816	-970.57	274.57	0.7792	-426.59	264.32	0.7265
s10	289.69	196.75	0.6845	-547.4	172.4	0.6872	-251.83	169.45	0.6466
s11	470.3	254.4	0.7665	-604.77	222.35	0.7678	-154.8	213.3	0.7109
s12	634.06	260.88	0.663	-454.3	227.2	0.6595	86.84	212.59	0.5774
s13	1604.43	165.16	0.0962	877.71	146.22	0.0992	1091.83	145.93	0.09898
s14	284.53	227.73	0.7216	-674	198.8	0.7244	-314.58	193.32	0.6705
s15	759.55	169.9	0.712	50.56	147.93	0.7062	329.34	143.73	0.7009
s16	-115.51	324.64	0.5556	-1452.8	281.55	0.551	-936.29	273.84	0.5116
s17	1066.24	159.43	0.3695	386.22	139.73	0.3734	591.9	139.2	0.3682
s18	205.14	231.75	0.7922	-769.04	202.3	0.7888	-373.72	195.12	0.7367

s19	-53.11	218.83	0.8075	-970.93	190.89	0.8034	-595.31	184.21	0.7505
s20	206.12	279.09	0.7442	-969.59	243.75	0.7419	-563.76	240.24	0.7204
s21	431.1	247	0.7022	-594.89	214.79	0.6948	-161.87	206.22	0.6442
s22	222.58	353.36	0.5528	-1245.98	307.3	0.5476	-684.15	299.37	0.521
s23	-849.98	415.56	0.7452	-2599.7	362.89	0.7425	-1957.21	354.74	0.7135
s24	688.27	269.71	0.645	-441.08	235.14	0.6407	1.687	227.918	0.6024
s25	110.01	264.86	0.6135	-1032.62	233.12	0.6161	-622.71	226.53	0.5826
s26	880.98	210.55	0.5416	-18.89	184.73	0.5452	311.9	180.1	0.5149
s27	842.44	259	0.6527	-247.76	226.11	0.6501	116.85	223.99	0.6279
s28	152.46	210.75	0.6997	-736.09	184.1	0.6976	-449.56	183.23	0.6853
s29	91.29	240.16	0.5987	-917.16	209.53	0.5982	-520.3	202.8	0.5759
s30	471.62	207.06	0.5109	-393.57	180.42	0.5093	-79.47	176.82	0.4833
s31	294.87	138.08	0.677	-278.21	120.05	0.6775	-66.13	117.16	0.6187
s32	-16.63	326.13	0.4329	-1395.95	285.19	0.435	-788.83	271.92	0.4012
s33	397.17	203.96	0.4159	-492.22	180.07	0.4298	-59.45	167.49	0.3686
s34	213.64	252.3	0.559	-864.1	221.3	0.562	-496.52	218.63	0.5317
s35	47.37	208.67	0.8244	-834.97	182.49	0.8218	-467.14	175.49	0.7567

Table 9.

Results of the correlation of tangential velocity and the one-third root of curvature per subject for experiment two.

Subject	Mean r^2	Minimum	Maximum
s1	0.0006	0.0000	0.0161
s2	0.0003	0.0000	0.0045
s3	0.0006	0.0000	0.0222
s4	0.0006	0.0000	0.0082
s5	0.0006	0.0000	0.0077
s6	0.0003	0.0000	0.0047
s7	0.0003	0.0000	0.0024
s8	0.0007	0.0000	0.0151
s9	0.0005	0.0000	0.0119
s10	0.0004	0.0000	0.0070
s11	0.0003	0.0000	0.0032
s12	0.0006	0.0000	0.0078
s13	0.0005	0.0000	0.0046
s14	0.0005	0.0000	0.0052
s15	0.0008	0.0000	0.0122
s16	0.0007	0.0000	0.0141
s17	0.0005	0.0000	0.0054
s18	0.0008	0.0000	0.0115
s19	0.0006	0.0000	0.0056

s20	0.0007	0.0000	0.0156
s21	0.0004	0.0000	0.0069
s22	0.0005	0.0000	0.0128
s23	0.0007	0.0000	0.0079
s24	0.0006	0.0000	0.0108
s25	0.0002	0.0000	0.0016
s26	0.0006	0.0000	0.0217
s27	0.0004	0.0000	0.0061
s28	0.0004	0.0000	0.0061
s29	0.0004	0.0000	0.0119
s30	0.0005	0.0000	0.0046
s31	0.0008	0.0000	0.0193
s32	0.0002	0.0000	0.0031
s33	0.0007	0.0000	0.0118
s34	0.0007	0.0000	0.0101
s35	0.0005	0.0000	0.0106

Table 10.

Results of the correlation of experimental velocity and the predicted minimum jerk velocity and the mean absolute deviation of the experimental velocity from the predicted minimum jerk velocity for experiment two.

				Mean Absolute		
	Mean r^2	Minimum	Maximum	Deviation	Minimum	Maximum
s1	0.0123	0.0089	0.0161	0.4962	0.2385	0.8342
s2	0.0134	0.0097	0.0163	0.4070	0.2378	0.5985
s3	0.0134	0.0090	0.0177	0.3353	0.1358	0.5699
s4	0.0131	0.0091	0.0164	0.4070	0.2495	0.5970
s5	0.0132	0.0101	0.0181	0.3685	0.2090	0.5635
s6	0.0122	0.0090	0.0157	0.5197	0.3150	0.8175
s7	0.0130	0.0095	0.0171	0.4337	0.2417	0.7077
s8	0.0132	0.0090	0.0167	0.4620	0.2647	0.6961
s9	0.0128	0.0095	0.0163	0.3828	0.2275	0.6277
s10	0.0126	0.0091	0.0157	0.5289	0.2904	0.8322
s11	0.0126	0.0063	0.0168	0.3987	0.2324	0.6284
s12	0.0127	0.0091	0.0163	0.3940	0.2128	0.6378
s13	0.0126	0.0088	0.0157	0.3731	0.1664	0.6552
s14	0.0118	0.0070	0.0164	0.4845	0.3083	0.7151
s15	0.0130	0.0089	0.0160	0.5035	0.2881	0.7171
s16	0.0136	0.0092	0.0167	0.3954	0.2157	0.6456

s17	0.0119	0.0079	0.0151	0.4677	0.3247	0.6730
s18	0.0124	0.0084	0.0156	0.4795	0.2405	0.7986
s19	0.0110	0.0069	0.0141	0.5702	0.3202	0.8681
s20	0.0120	0.0077	0.0146	0.4185	0.2183	0.6253
s21	0.0129	0.0086	0.0164	0.3972	0.2352	0.6134
s22	0.0141	0.0086	0.0186	0.3316	0.1784	0.5371
s23	0.0134	0.0104	0.0171	0.3889	0.2062	0.6860
s24	0.0135	0.0058	0.0175	0.3686	0.1779	0.5324
s25	0.0127	0.0080	0.0167	0.4043	0.1629	0.6878
s26	0.0131	0.0099	0.0160	0.3835	0.1916	0.5605
s27	0.0132	0.0083	0.0186	0.3624	0.2057	0.5695
s28	0.0119	0.0076	0.0150	0.5360	0.2813	0.8099
s29	0.0119	0.0078	0.0159	0.5057	0.2484	0.9364
s30	0.0119	0.0072	0.0153	0.4402	0.2387	0.7575
s31	0.0112	0.0064	0.0143	0.7207	0.4010	1.1397
s32	0.0135	0.0086	0.0178	0.3619	0.1875	0.6722
s33	0.0130	0.0086	0.0163	0.4617	0.2318	0.8120
s34	0.0122	0.0089	0.0149	0.4563	0.2701	0.7291
s35	0.0126	0.0087	0.0156	0.5088	0.2907	0.8203

Figures

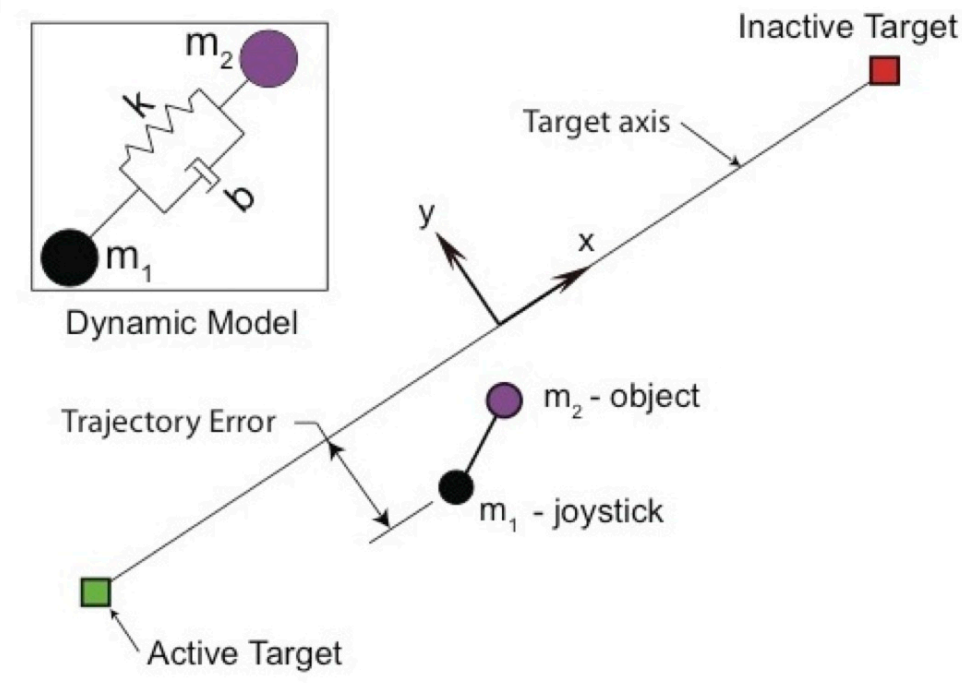

Figure 1. The properties of the spring-target task. M1 is the object that is controlled by the mouse. M2 is the item that has to hit the active target. The dynamic model shows the properties of the spring system.

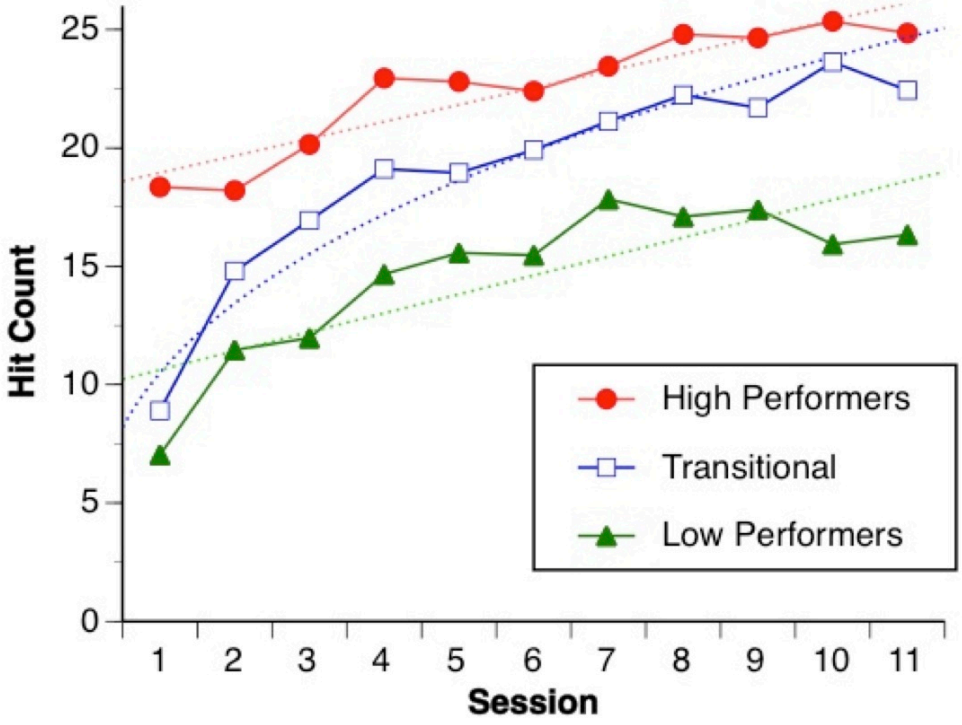

Figure 2. The mean hit count for the three different subject groups over session. The 11th session was a retention session.

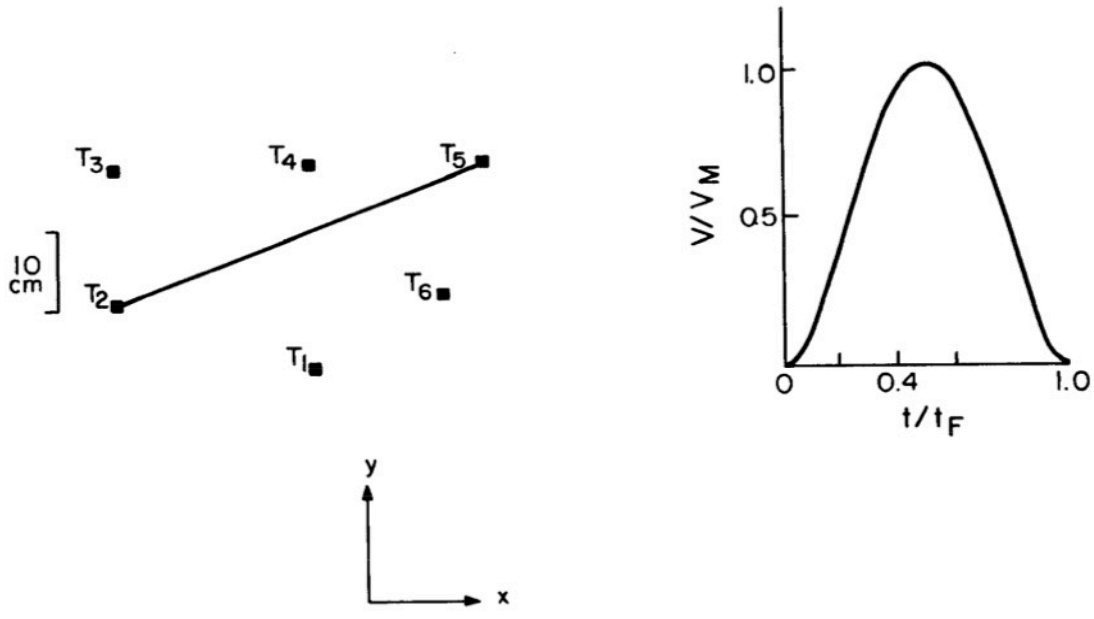

Figure 3. An example movement from Flash and Hogan (1985)

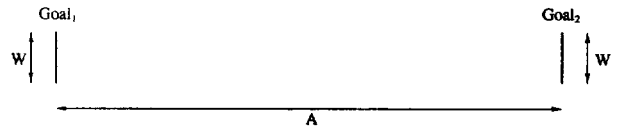

Figure 4, Goal passing task from Accot and Zhai (1997)

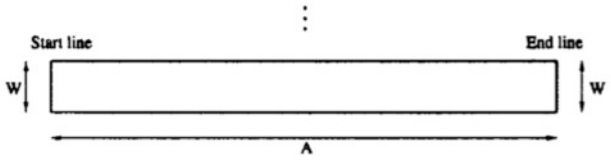

Figure 5. Straight tunnel task from Accot and Zhai (1997)

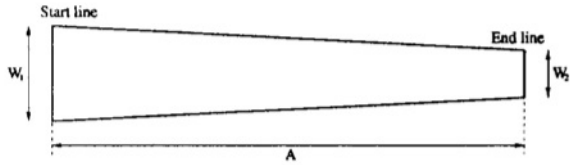

Figure 6. Narrowing tunnel task from Accot and Zhai (1997)

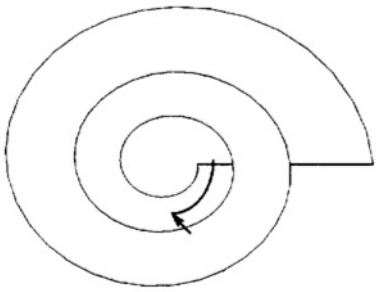

Figure 7. Spiral tunnel task from Accot and Zhai (1997)

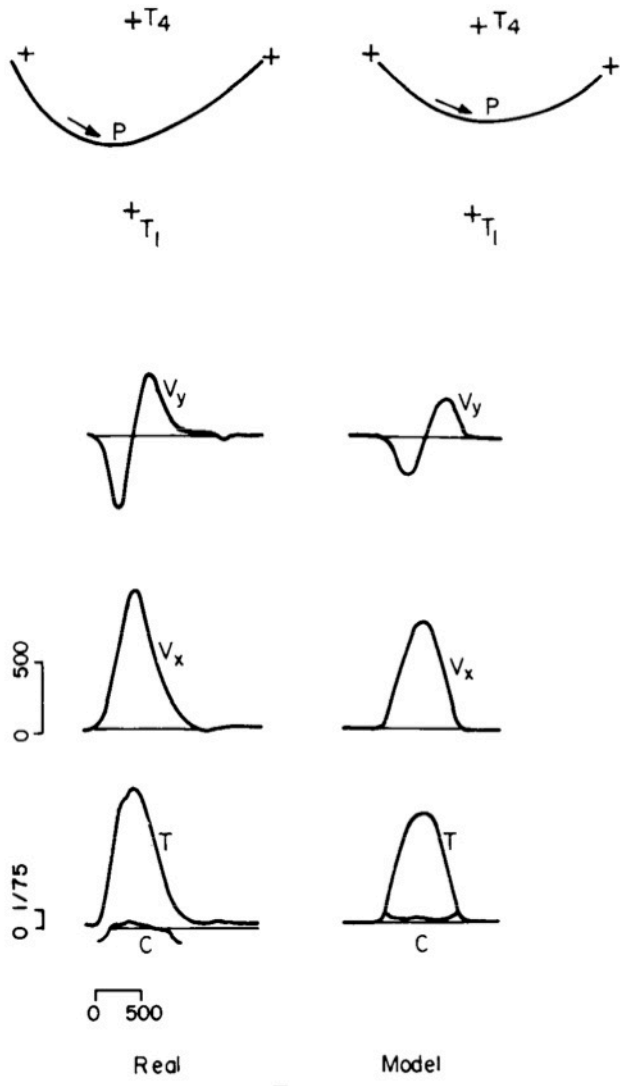

Figure 8. Representative examples between real and predicted movements in the way point experiment. The top is the hand paths and plots of the hand speed, T, curvature, C, and velocity components versus time.

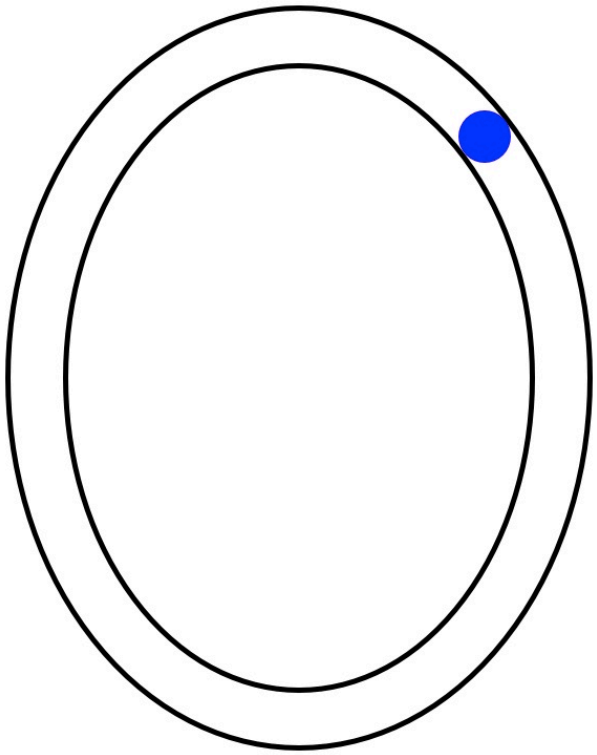

Figure 9. Example trial from experiment one

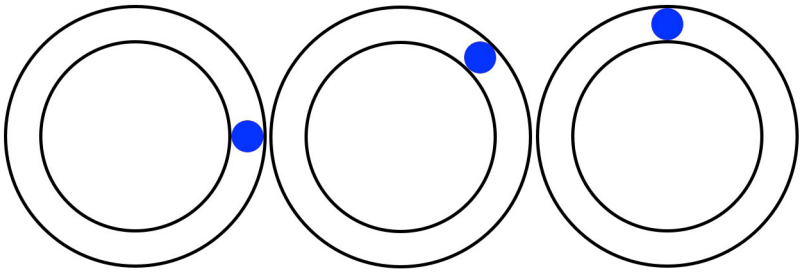

Figure 10. Illustration of the three start positions for experiment one. From left to right they are 0°, 45°, and 90°.

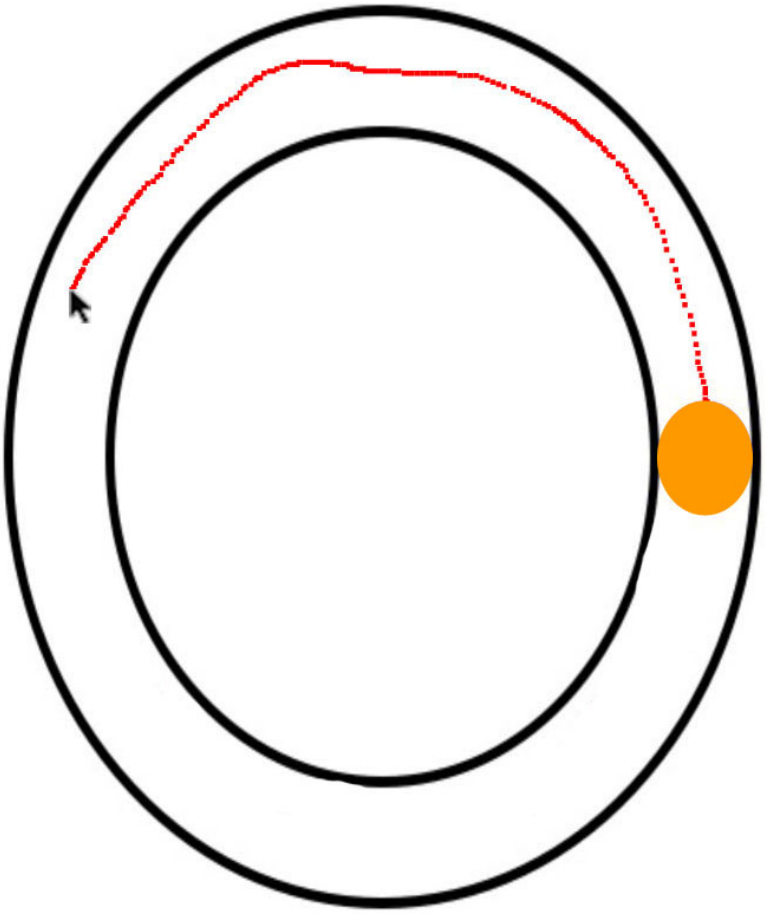

Figure 11. An example trial from experiment one in progress. The red dots represent the trajectory that the subject took and are not visible to the subject while the trial is in progress.

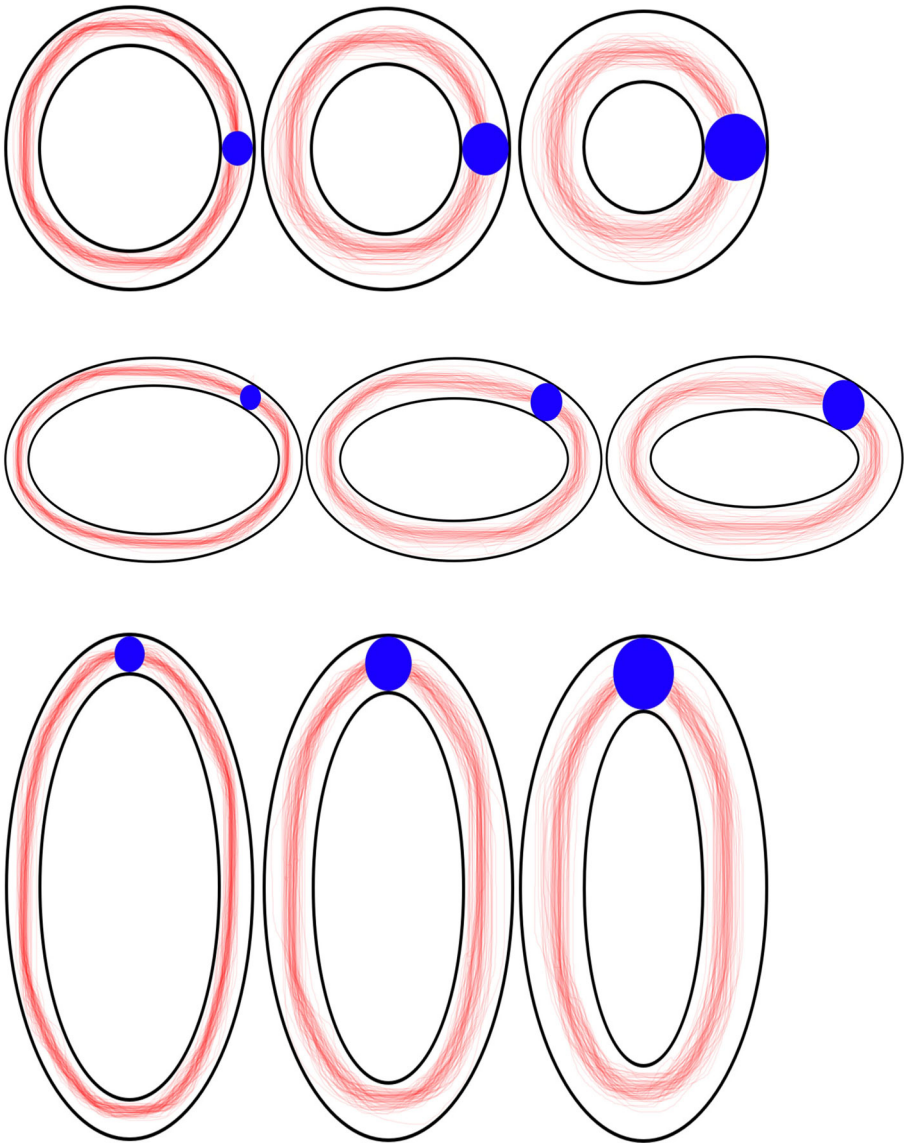

Figure 12. The aggregated trajectories for all subjects on 9 different trials in experiment one. The first column is the smallest path width, the second is the middle path width, and the third is the longest path width. The top row of trials is the smallest circle at start position 0 degrees. The second row of trials is the widest ellipse at start position 45 degrees. The third row of trials is the tallest ellipse with a start position of 90 degrees.

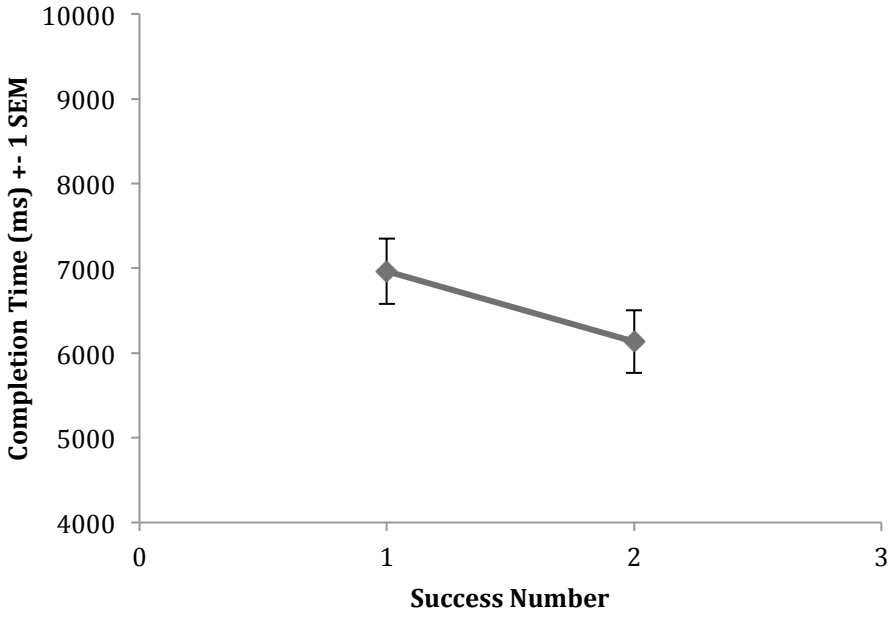

Figure 13. The mean completion time for experiment one across the two successful trials.

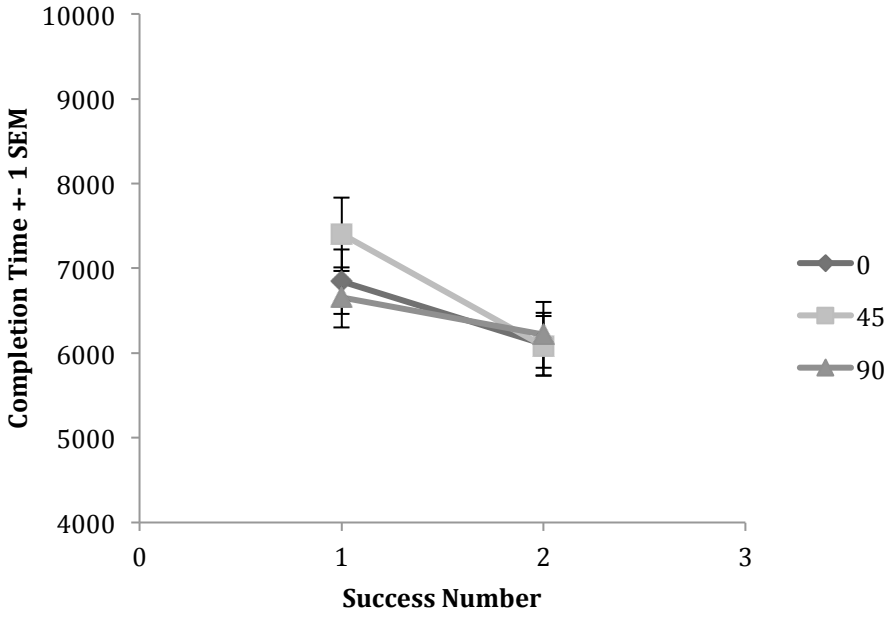

Figure 14. The mean completion time for experiment one for the two successes separated by start position.

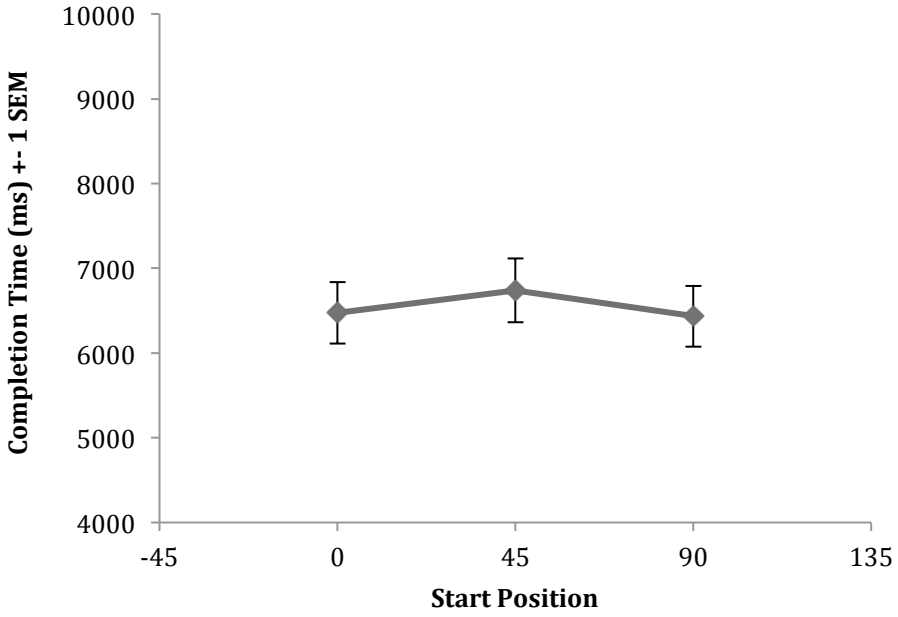

Figure 15. The mean completion time for experiment one across the three different starting positions.

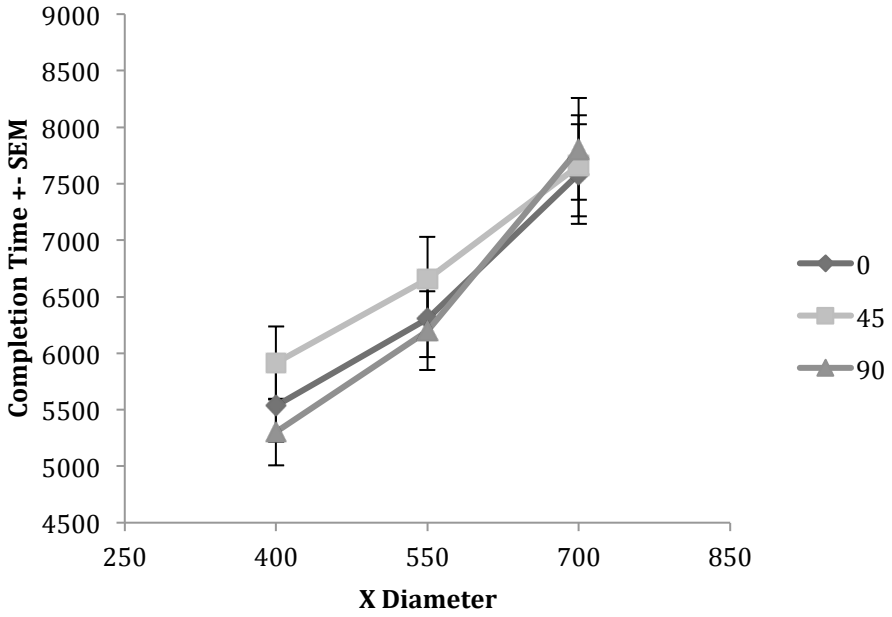

Figure 16. The mean completion time for experiment one across the three X diameters separated by start position.

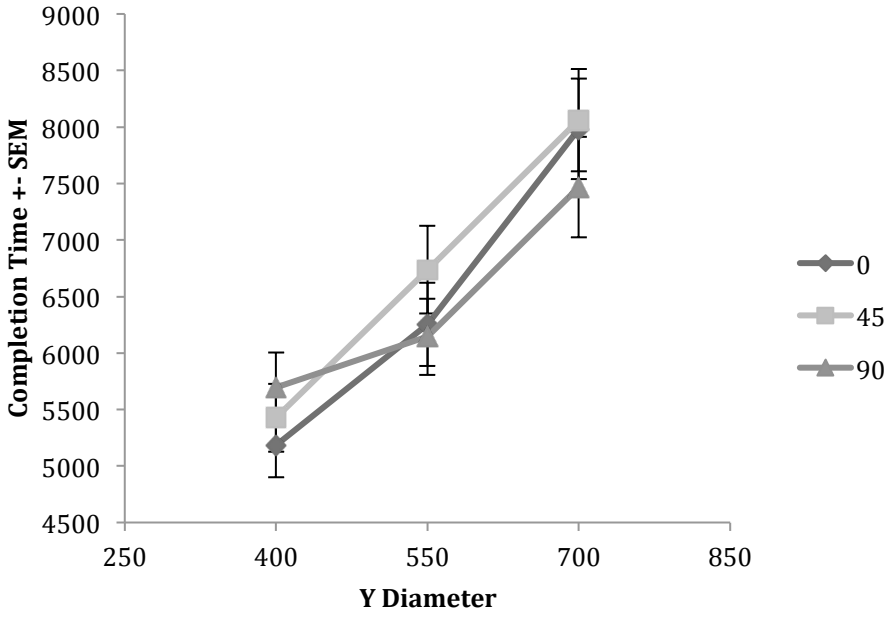

Figure 17. The mean completion time for experiment one across the three Y diameters separated by start position.

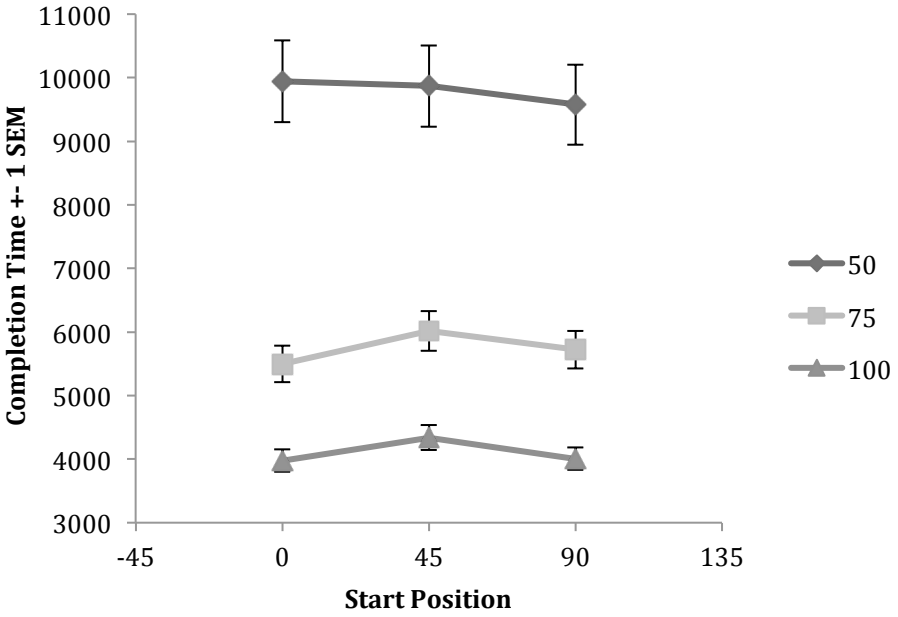

Figure 18. The mean completion time for experiment one across the three start positions separated by the path width.

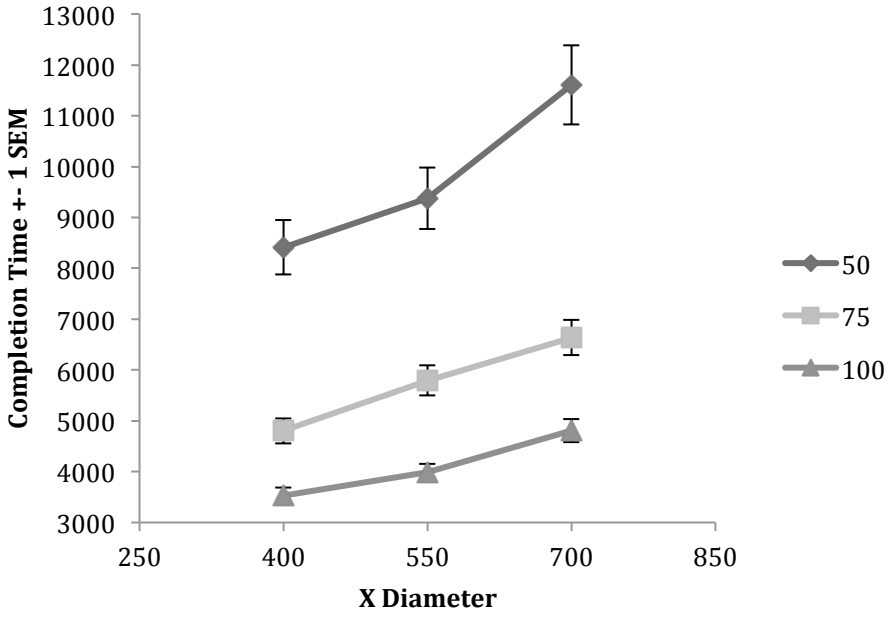

Figure 19. The mean completion time for experiment one across the three X diameters separated by the path width.

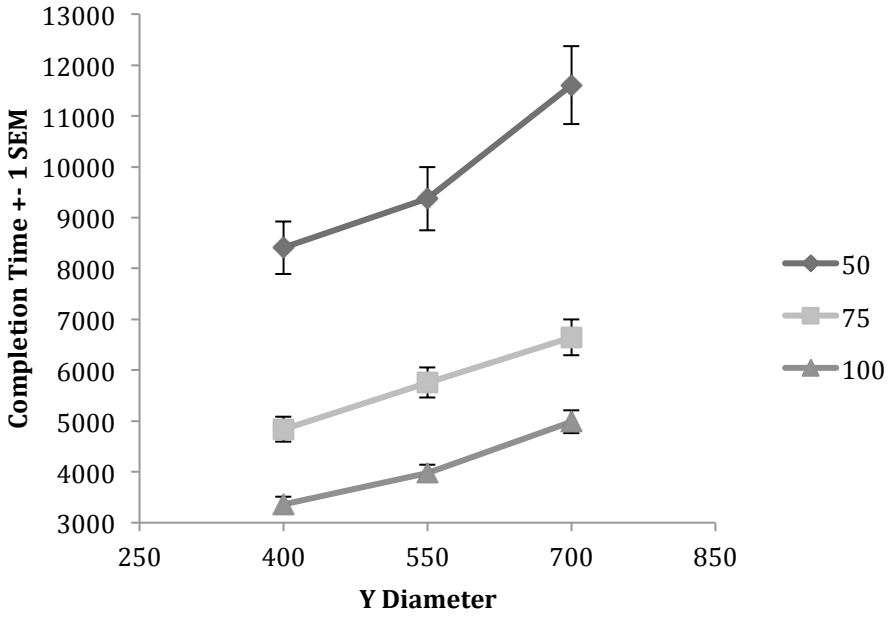

Figure 20. The mean completion time for experiment one across the three Y diameters separated by path width.

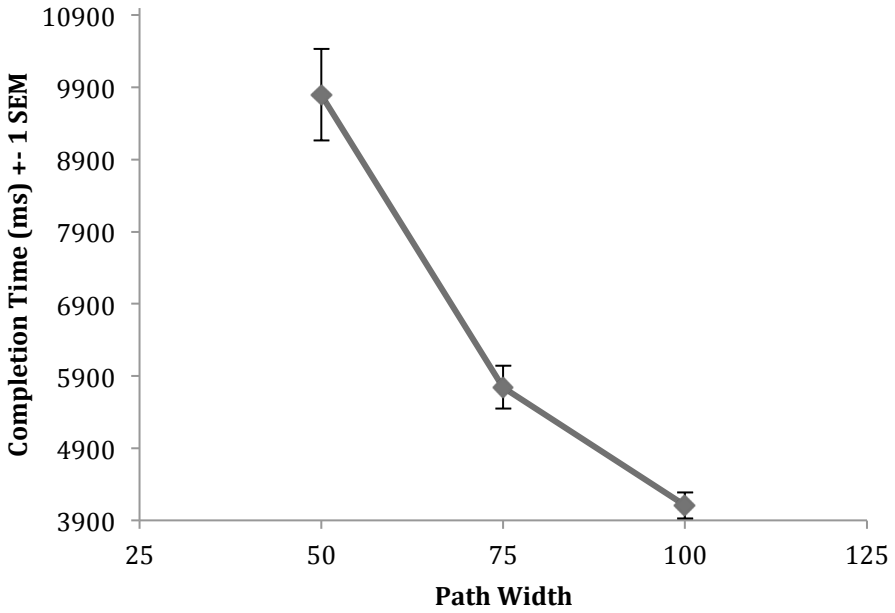

Figure 21. The mean completion time for experiment one across the three different path widths.

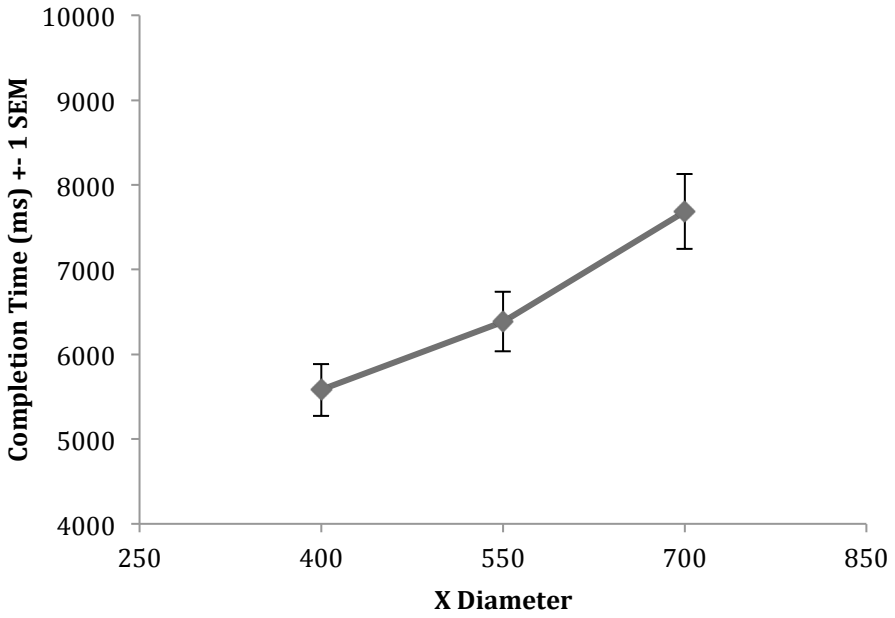

Figure 22. The mean completion time for experiment one across the three different X Diameters.

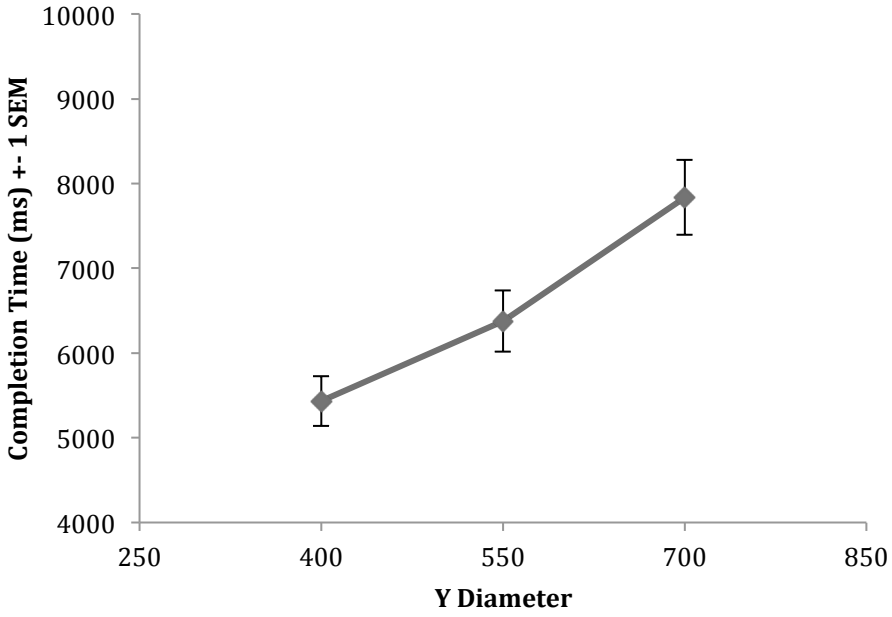

Figure 23. The mean completion time for experiment one across the three different Y Diameters.

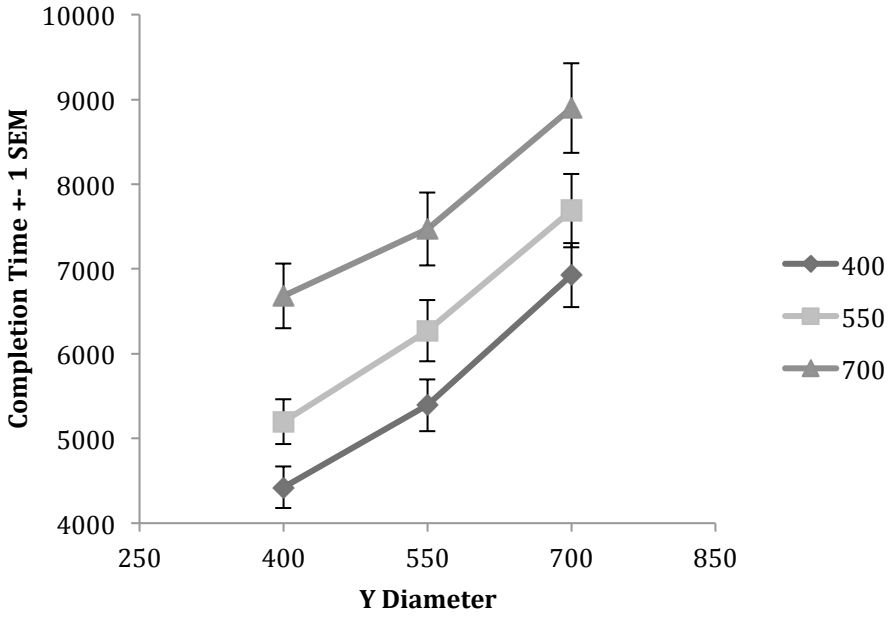

Figure 24. The mean completion time for experiment one across the three Y diameters separated by X diameter.

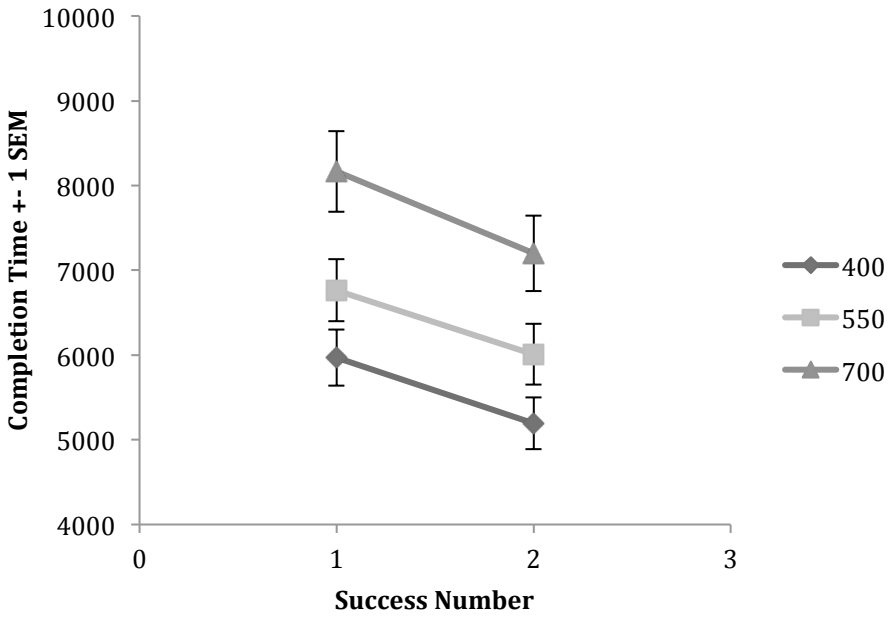

Figure 25. The mean completion time for experiment one for the two successes separated by X diameter.

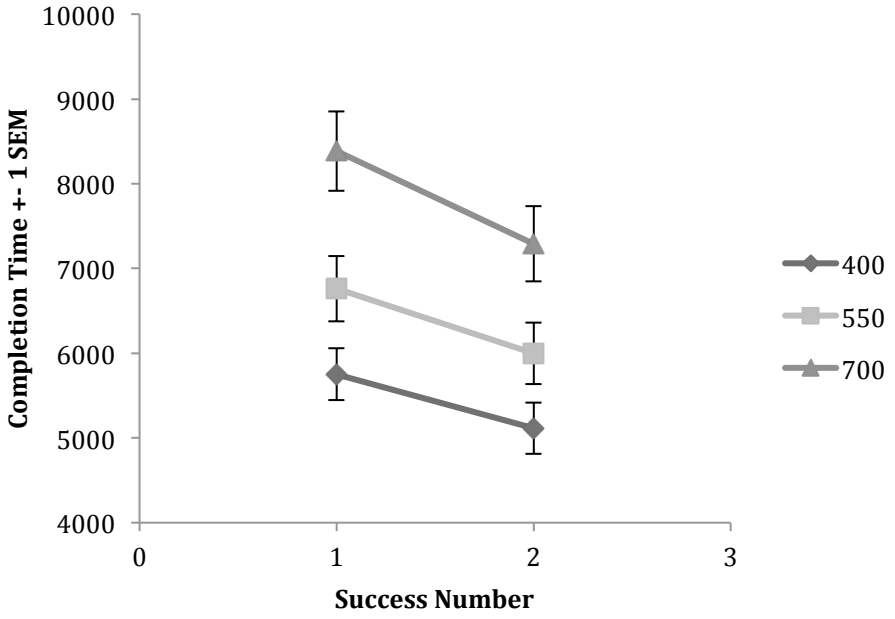

Figure 26. The mean completion time for experiment one for the two successes separated by Y diameter.

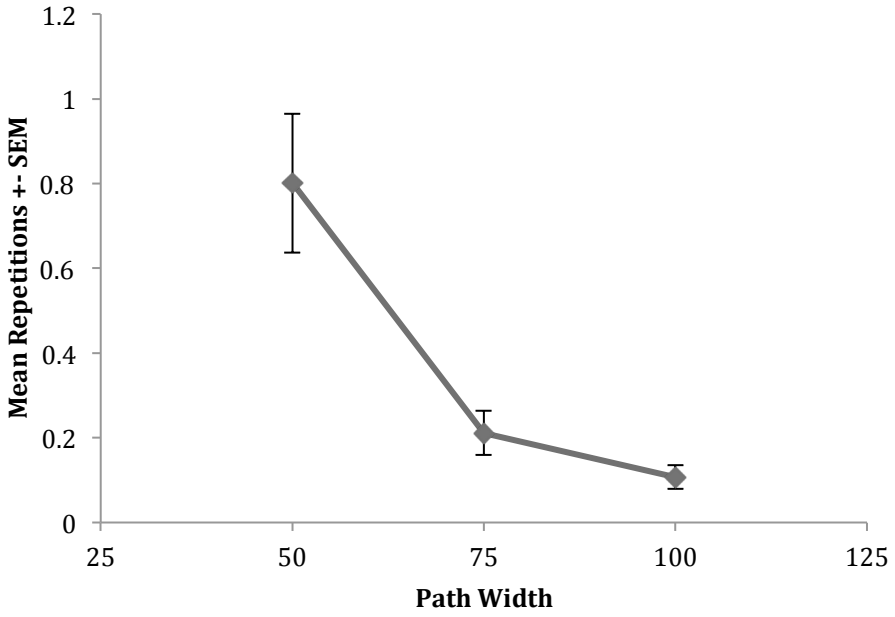

Figure 27. The mean repetition for experiment one across the three path widths.

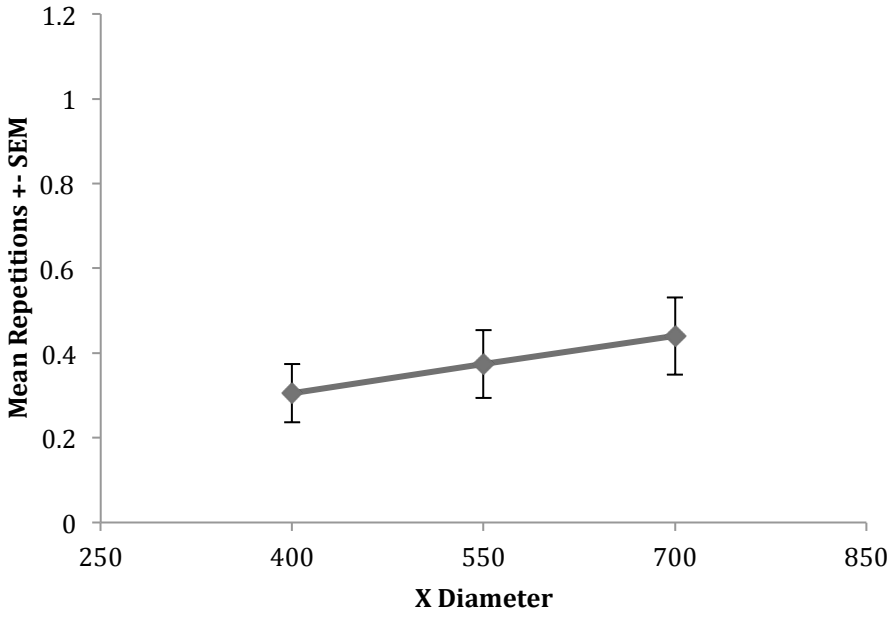

*Figure 28.*The mean repetition for experiment one across the three x diameters.

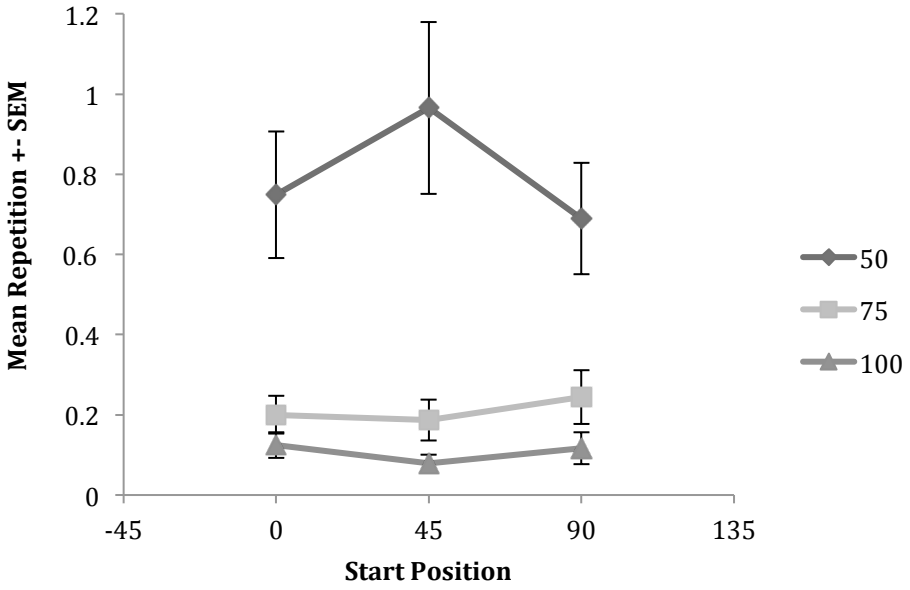

Figure 29. The mean repetitions for experiment one across the three start positions separated by path width.

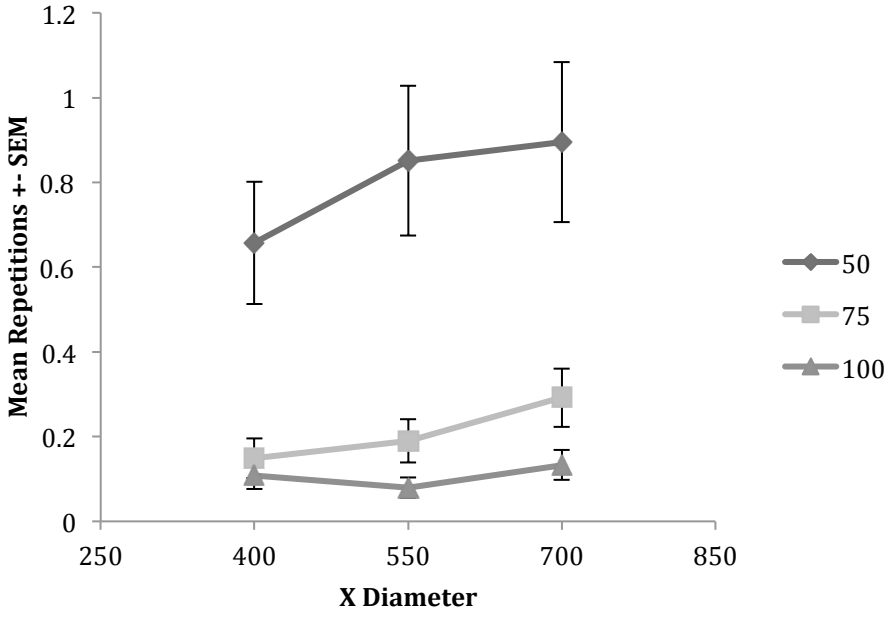

Figure 30. The mean repetitions for experiment one across the three X diameters separated by path width

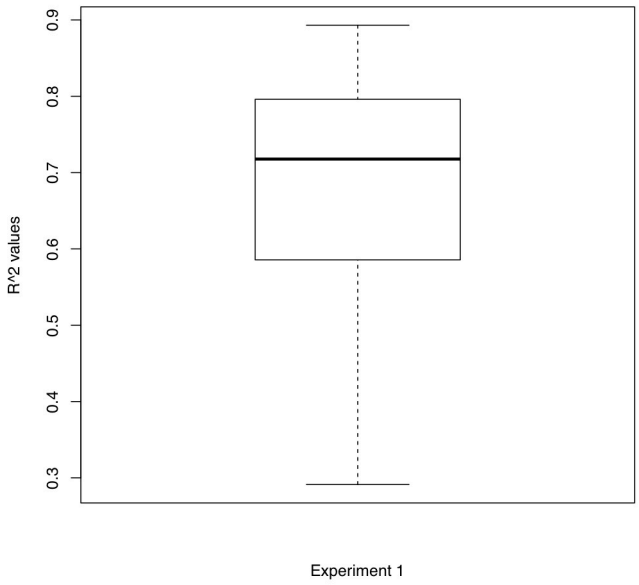

Figure 31. The distribution of r^2 values for experiment one Fitts's Law analysis.

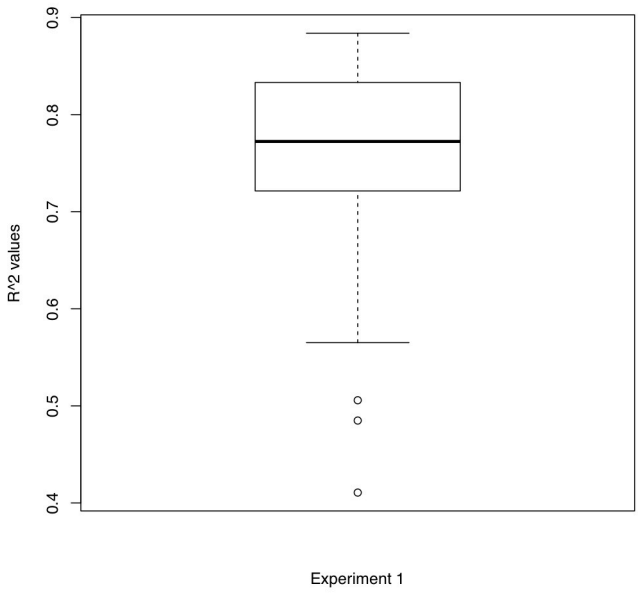

Figure 32. The distribution of r^2 values for experiment one success two trials Fitts's Law analysis.

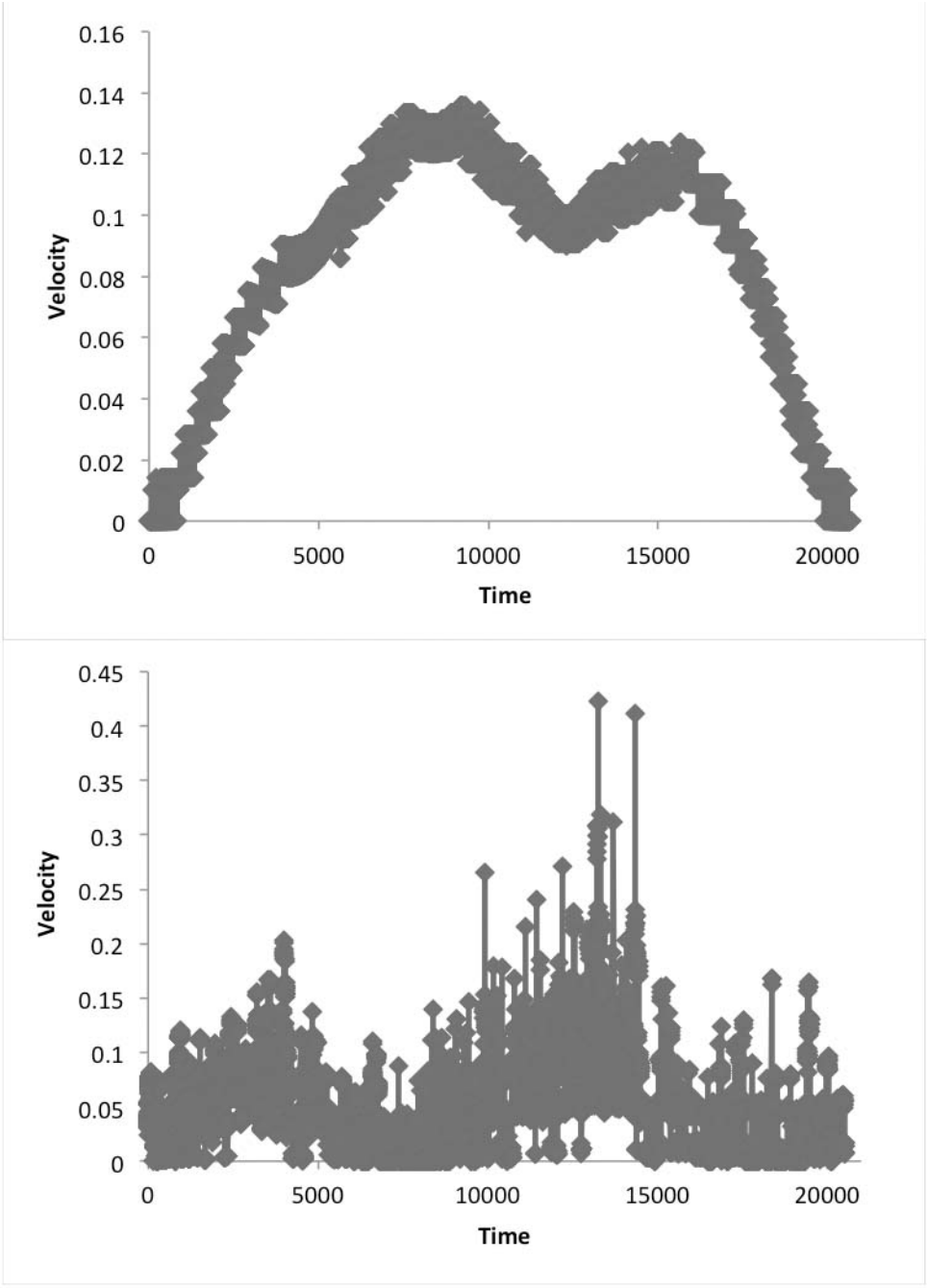

Figure 33. Velocity graphs for the trial with the highest r^2 value in experiment one. Top graph is the predicted velocity using the minimum jerk profile. The bottom graph is the subject's velocity over time for the trial.

Figure 34. Example trial from experiment two

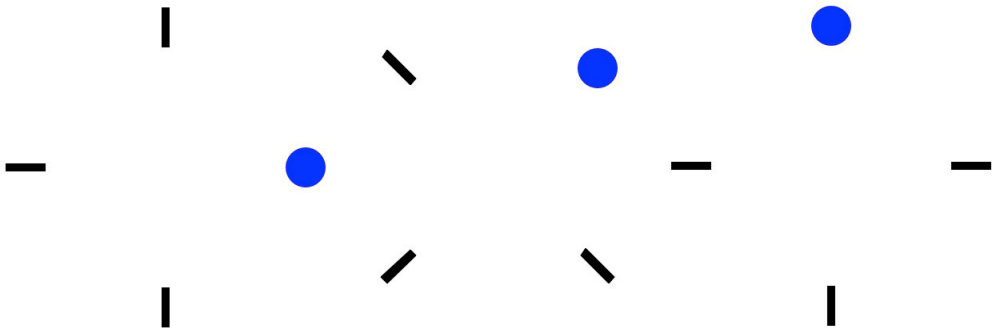

Figure 35. Illustration of the three start positions for experiment two. From left to right they are 0°, 45°, and 90°.

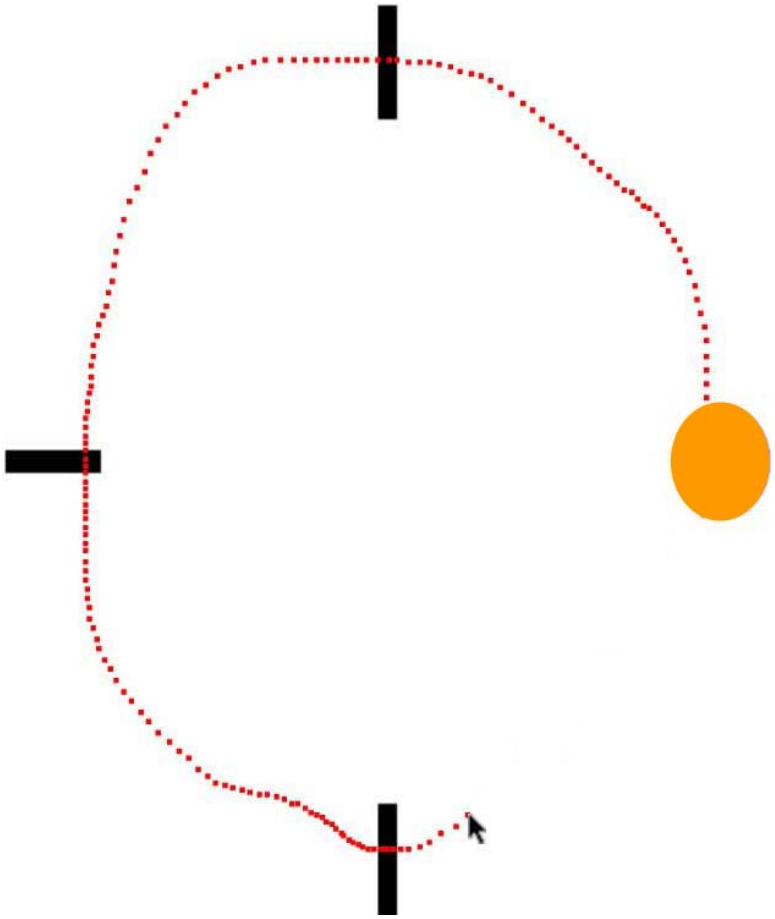

Figure 36. An example of a trial in progress from experiment two. The red dots are the trajectory that the subject took and are not visible to the subject.

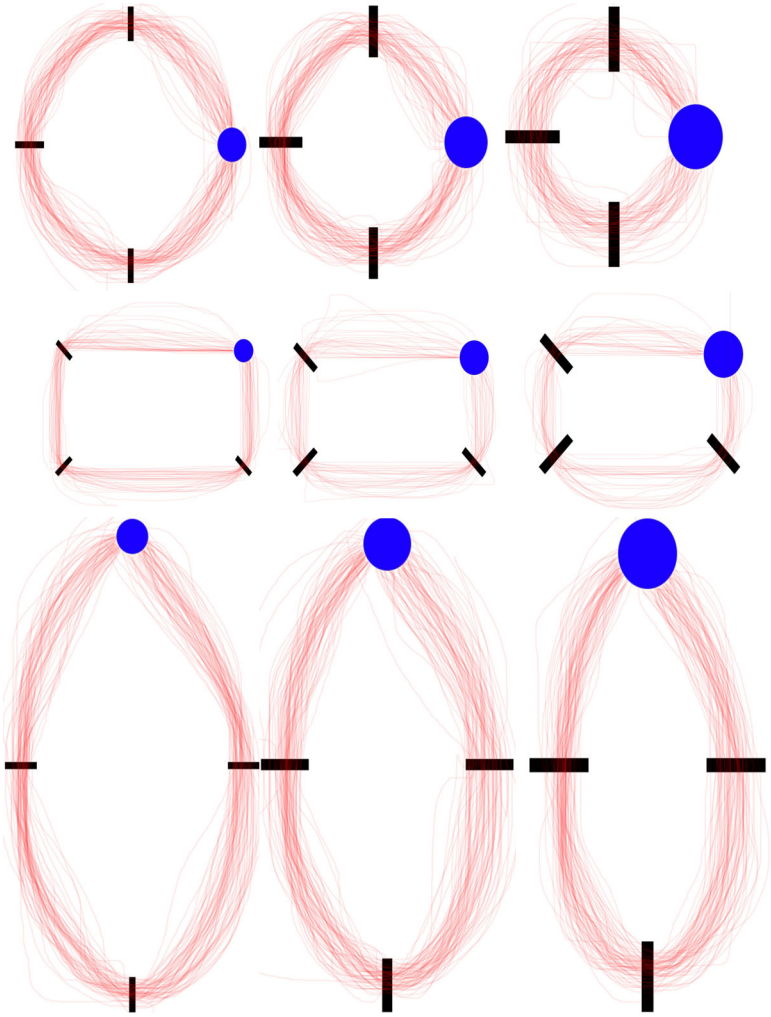

Figure 37. The aggregated trajectories for all subjects on 9 different trials in experiment two. The first column is the smallest path width, the second is the middle path width, and the third is the longest path width. The top row of trials is the smallest circle at start position 0 degrees. The second row of trials is the widest ellipse at start position 45 degrees. The third row of trials is the tallest ellipse with a start position of 90 degrees.

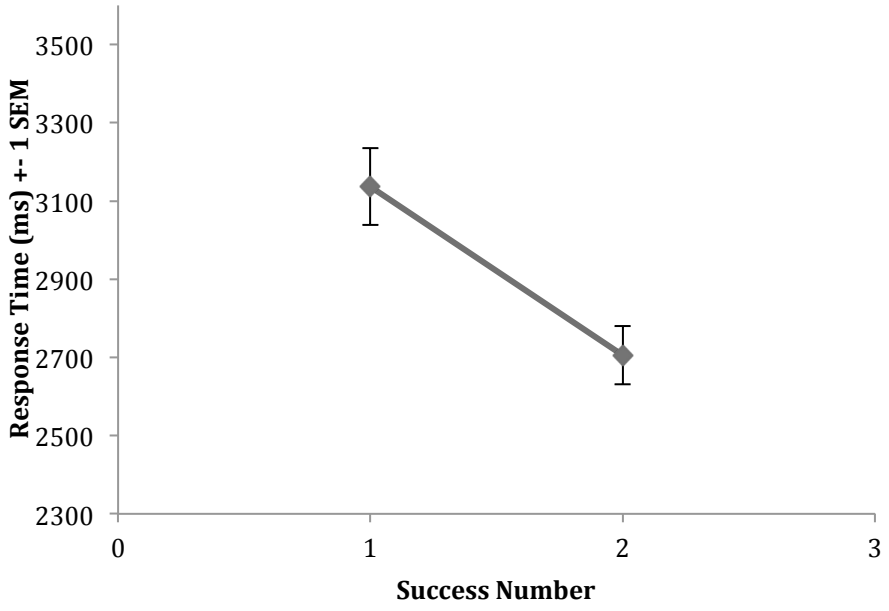

Figure *38.* The mean completion time for experiment two across the two successful trials.

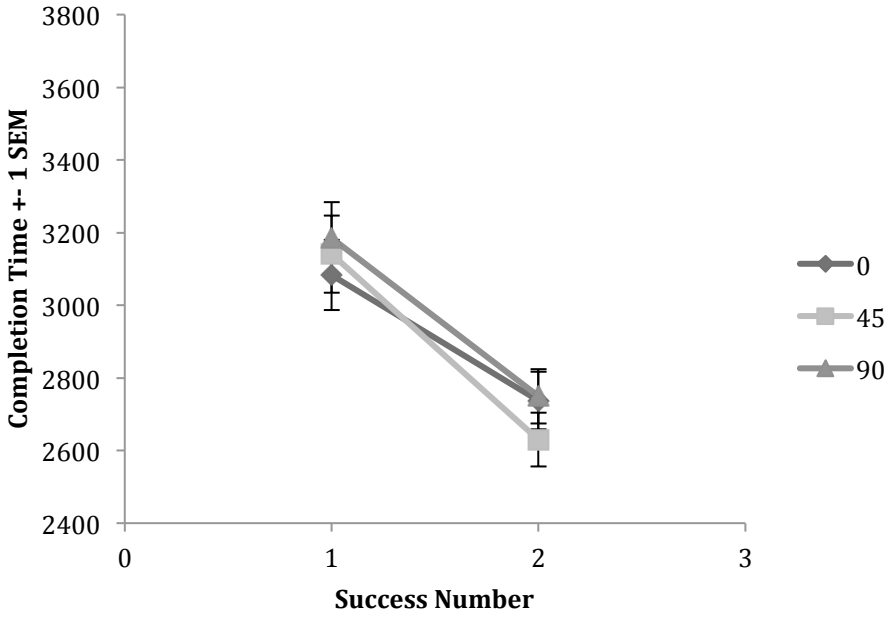

Figure 39. The mean completion time for experiment two for the two successes separated by start position.

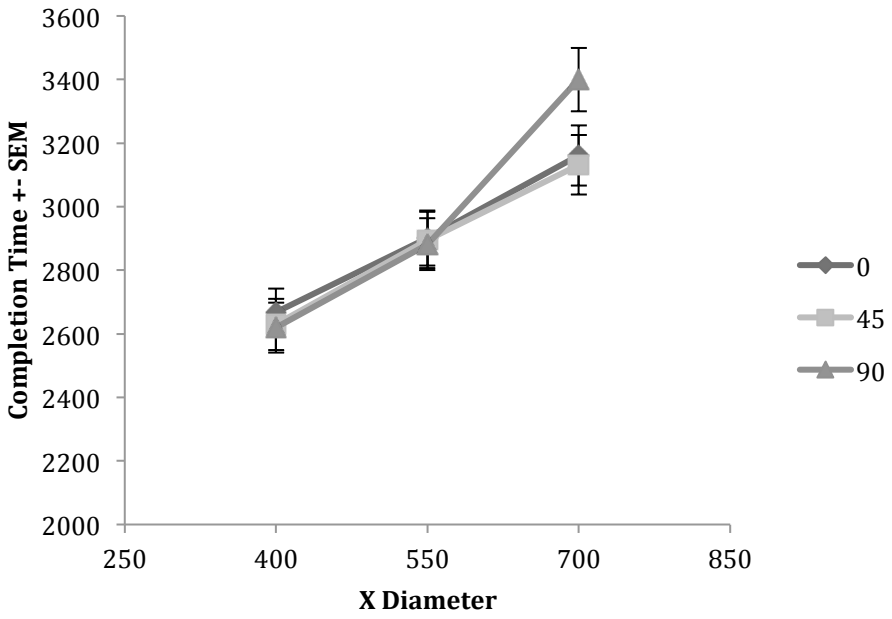

Figure 40. The mean completion time for experiment two across the three X diameters separated by the starting position.

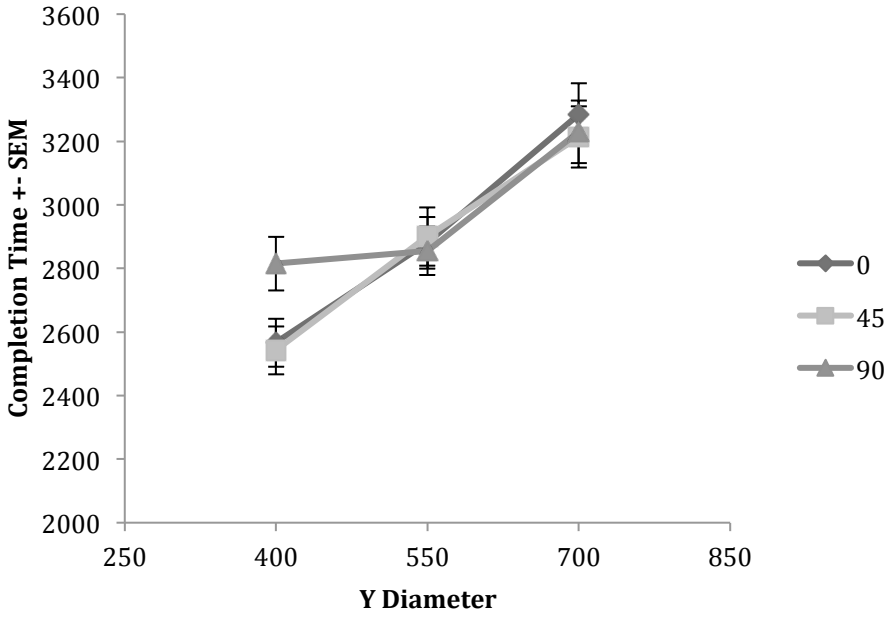

Figure 41. The mean completion time for experiment two across the three Y diameters separated by the starting position.

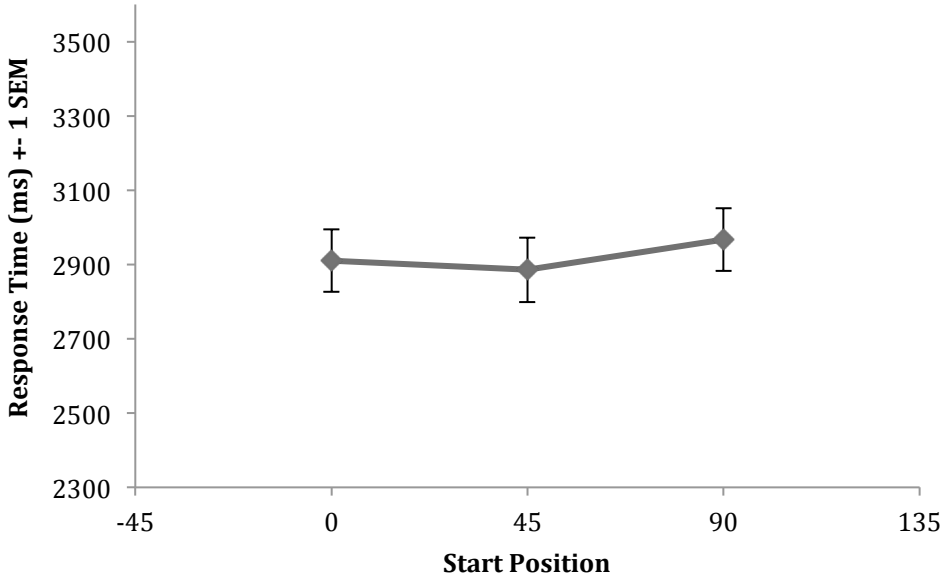

Figure 42. The mean completion time for experiment two across the three different starting positions.

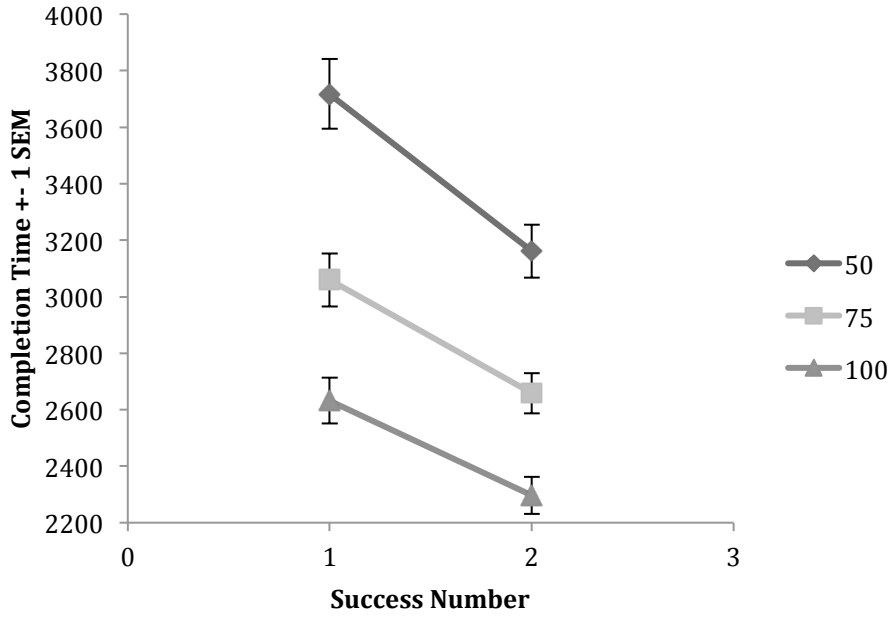

Figure 43. The mean completion time for experiment two for the two successes separated by gateway size.

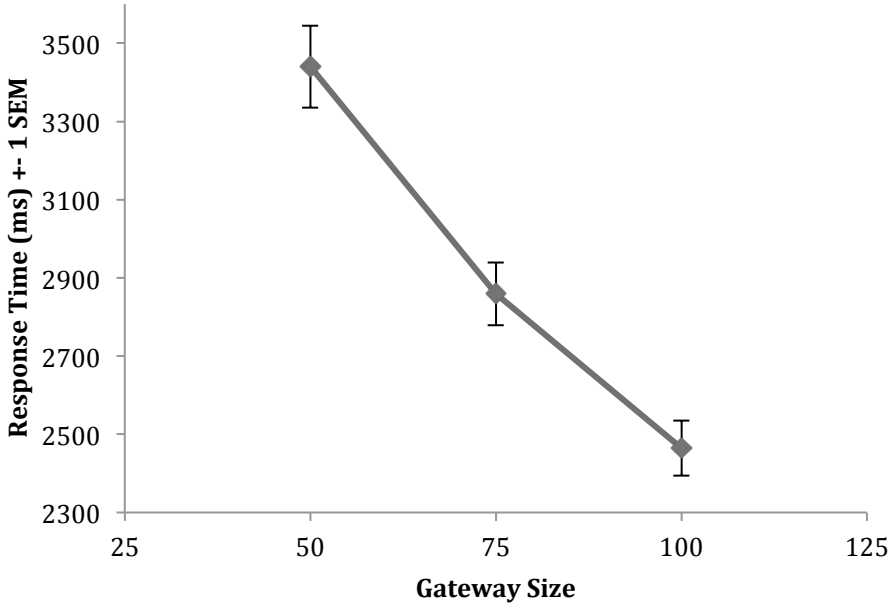

Figure 44. The mean completion time for experiment two across the three different gateway sizes.

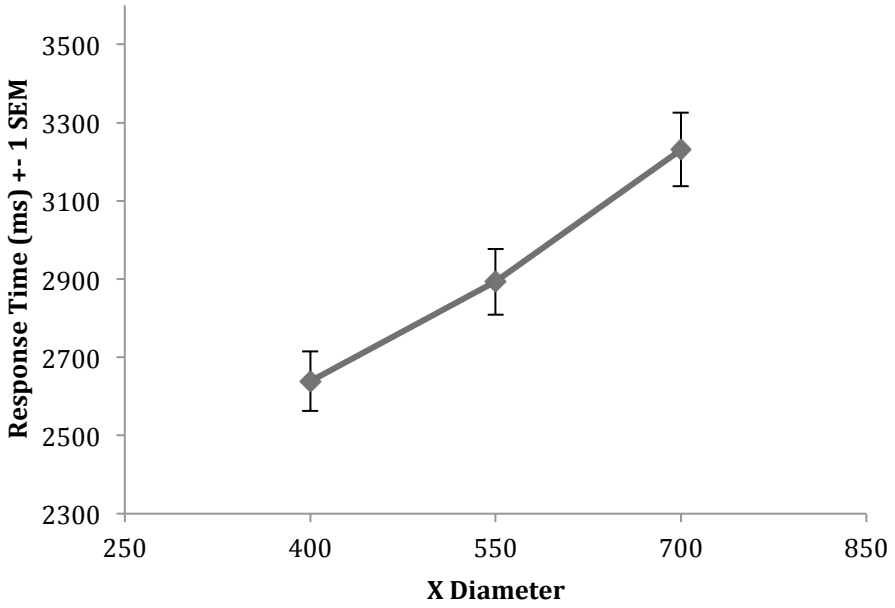

Figure 45. The mean completion time for experiment two across the three different X Diameters.

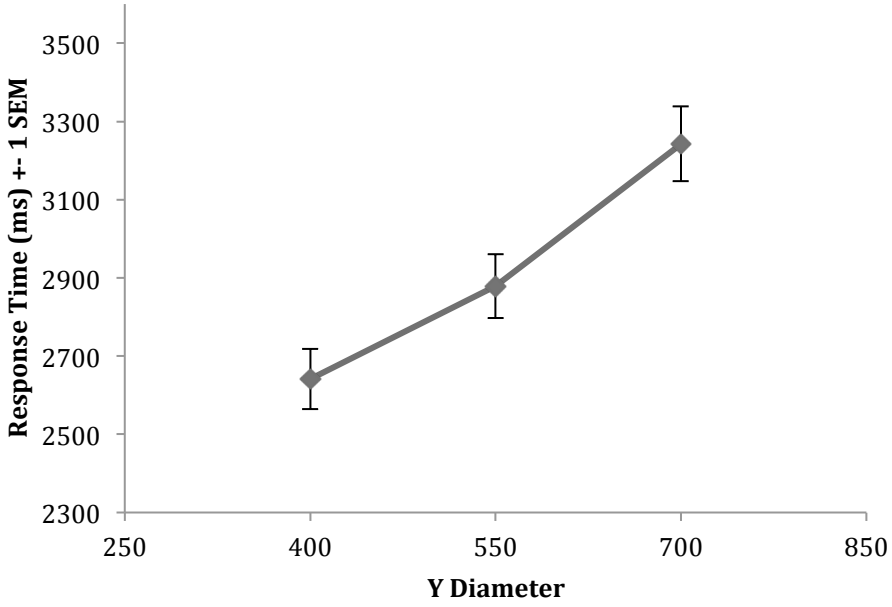

Figure 46. The mean completion time for experiment two across the three different Y Diameters.

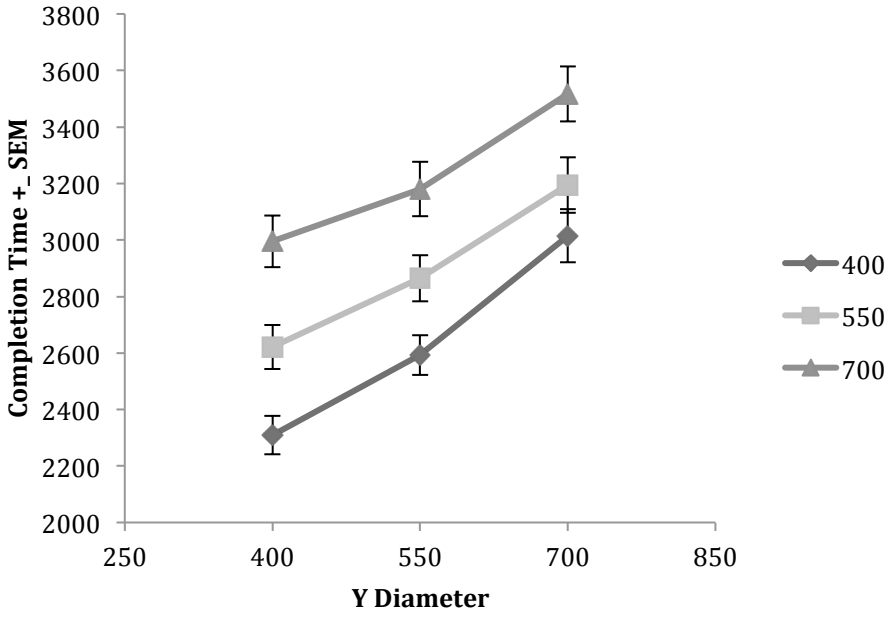

Figure 47. The mean completion time for experiment two across the different Y diameters separated by X diameter.

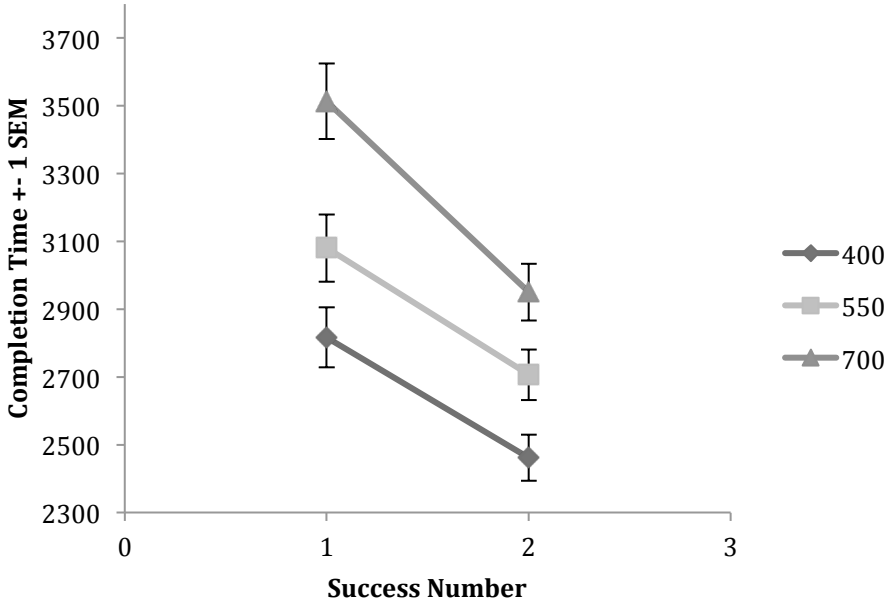

Figure 48. The mean completion time for experiment two for the two successes separated by X Diameter.

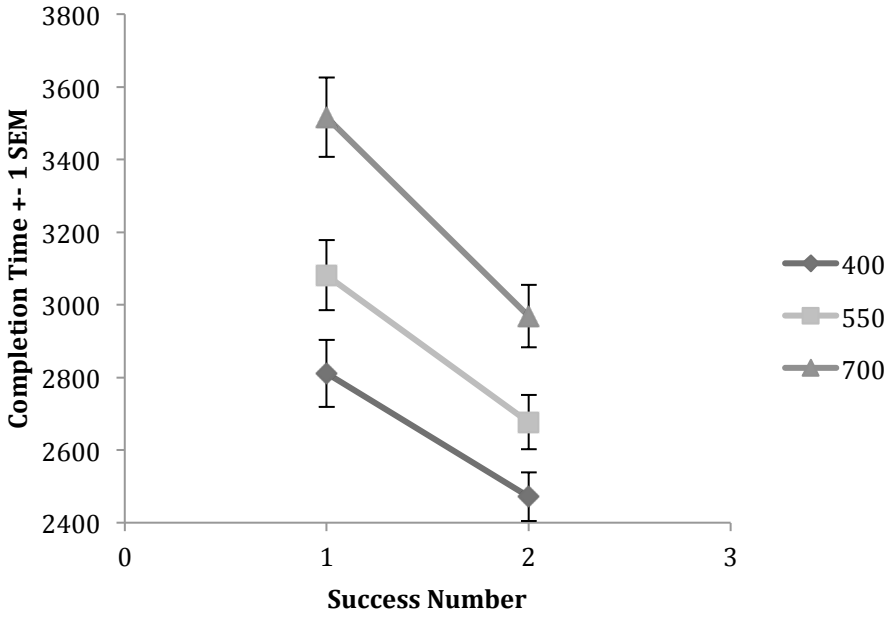

Figure 49. The mean completion time for experiment two for the two successes separated by Y Diameter

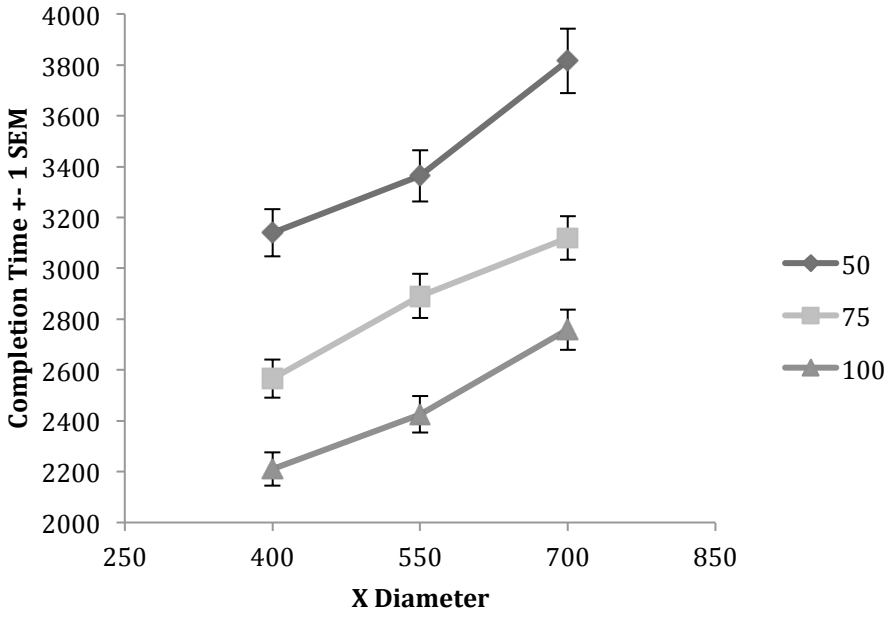

Figure 50. The mean completion time for experiment two across the three X diameters separated by the gateway size.

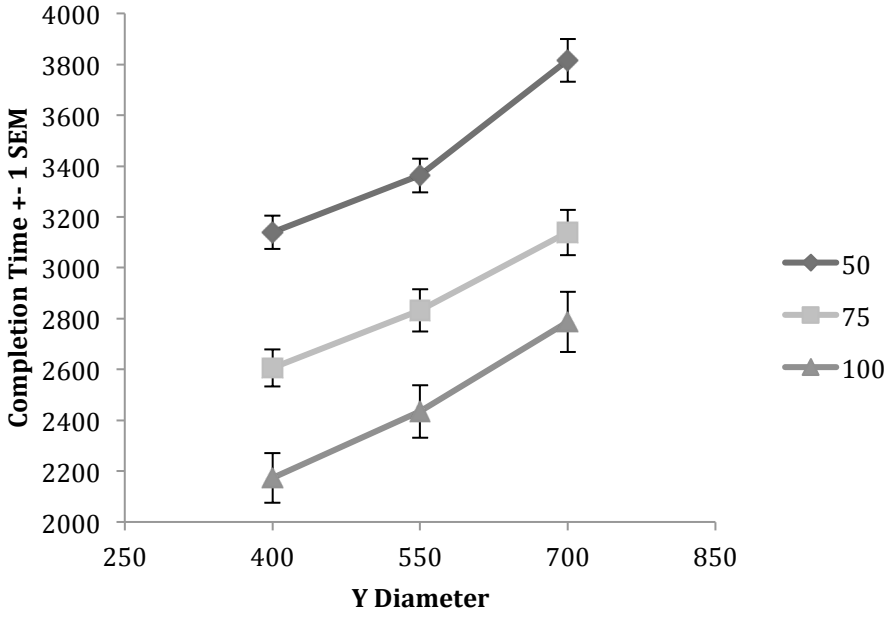

Figure 51. The mean completion time for experiment two across the three Y diameters separated by the gateway size.

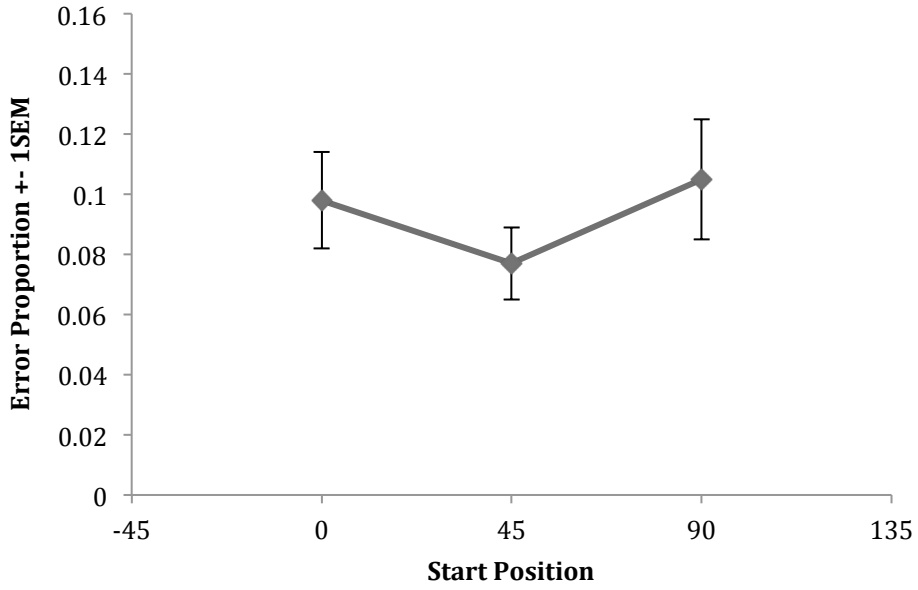

Figure 52. The error proportion in experiment two across the three start positions.

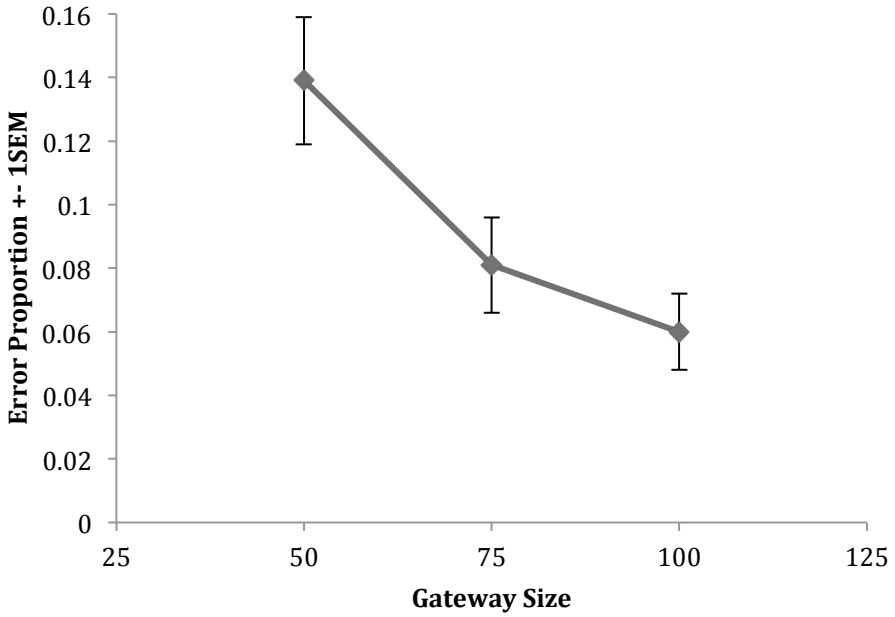

Figure 53. The error proportion in experiment two across the three gateway sizes.

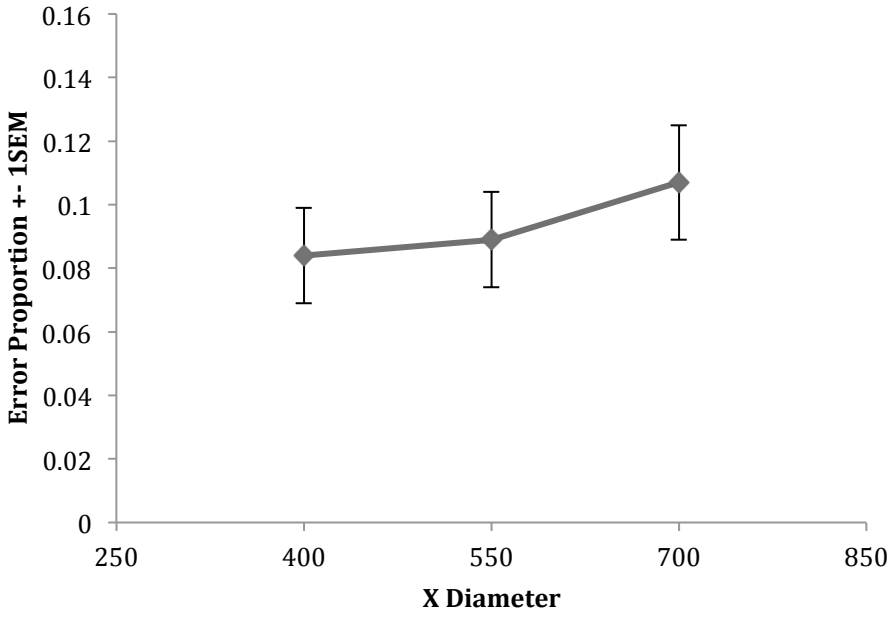

Figure 54. The error proportion in experiment two across the three X diameters.

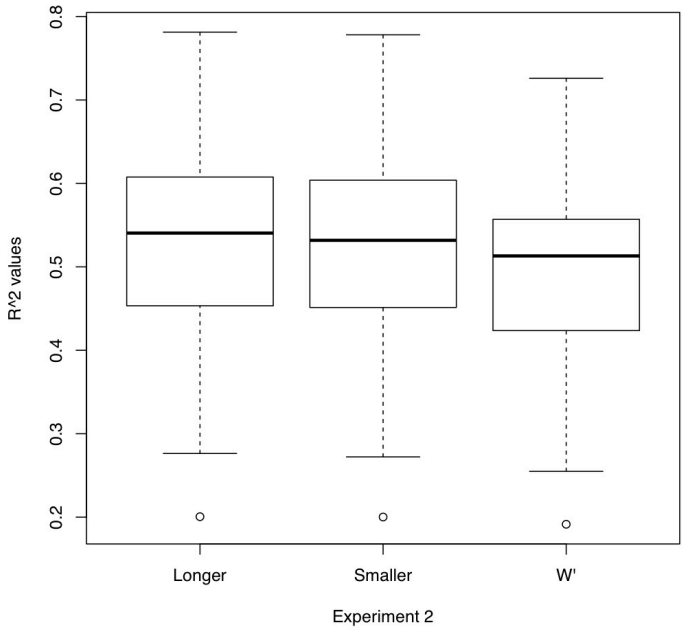

Figure 55. The distribution of r^2 values for the three indices of difficulty in experiment two.

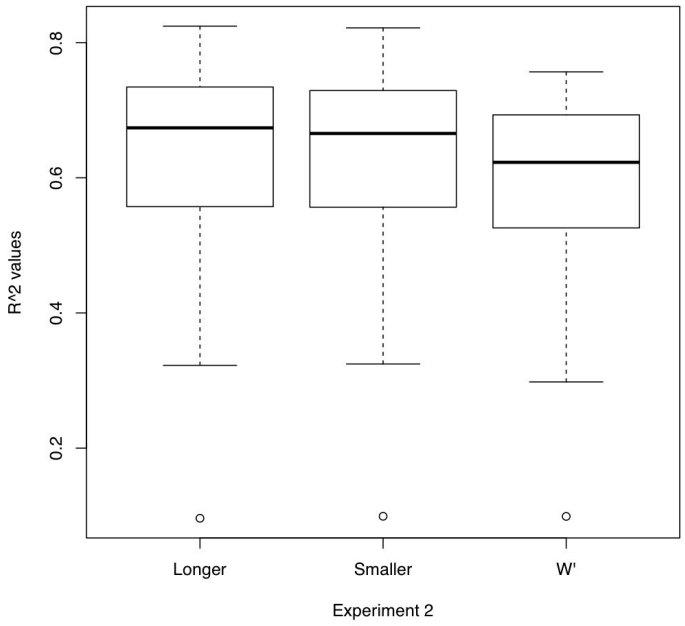

Figure 56. The distribution of r^2 values for the three indices of difficulty on the second success in experiment two.

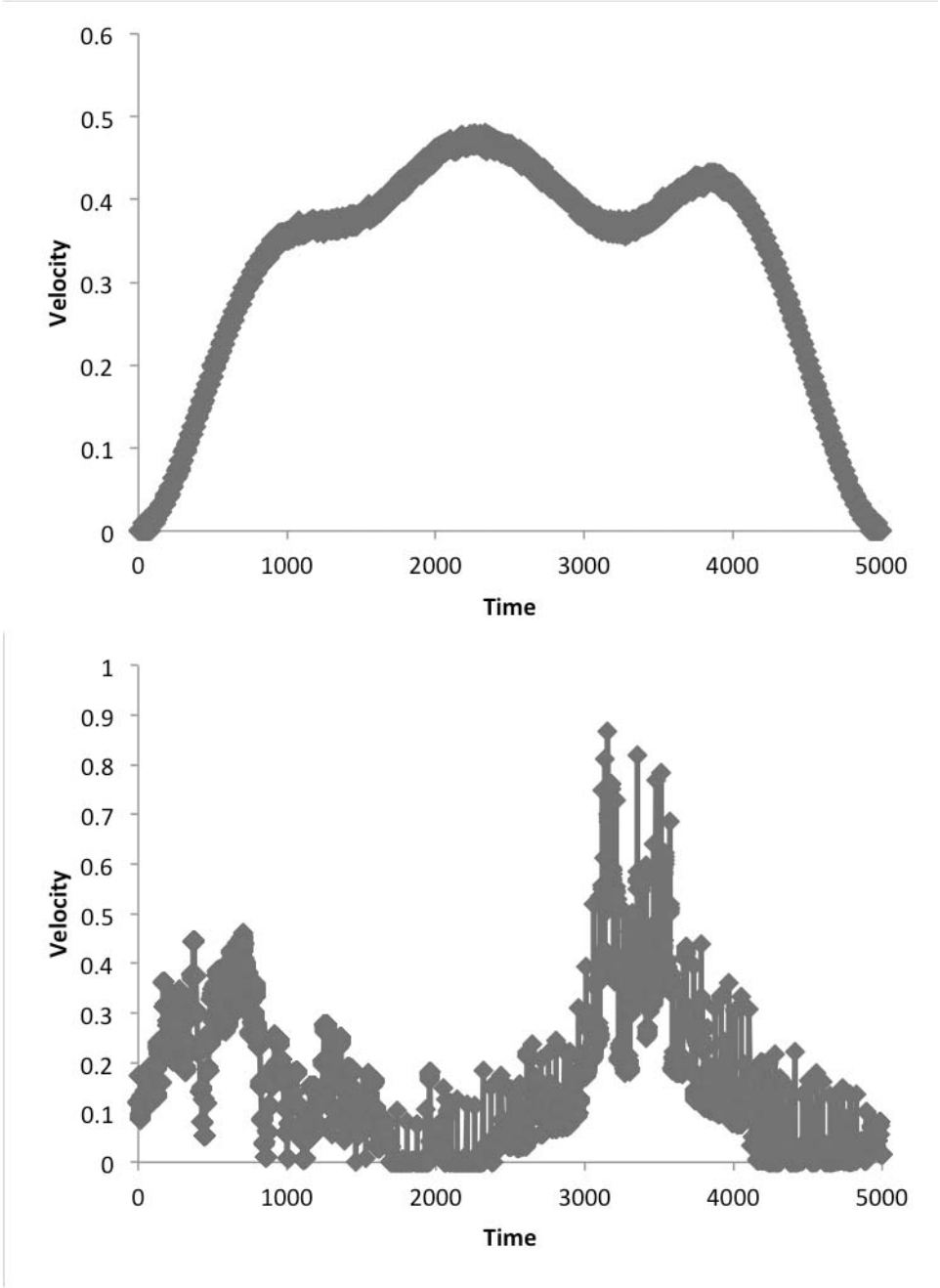

Figure 57. Velocity graphs for the trial with the highest r^2 value in experiment two. Top graph is the predicted velocity using the minimum jerk profile. The bottom graph is the subject's velocity over time for the trial.